



HAL
open science

Control of the Effects of Regularization on Variational Optic Flow Computations

Z Belhachmi, Frédéric Hecht

► **To cite this version:**

Z Belhachmi, Frédéric Hecht. Control of the Effects of Regularization on Variational Optic Flow Computations. *Journal of Mathematical Imaging and Vision*, 2011, 40 (1), 10.1007/s10851-010-0239-x . hal-01279861

HAL Id: hal-01279861

<https://hal.science/hal-01279861>

Submitted on 27 Feb 2016

HAL is a multi-disciplinary open access archive for the deposit and dissemination of scientific research documents, whether they are published or not. The documents may come from teaching and research institutions in France or abroad, or from public or private research centers.

L'archive ouverte pluridisciplinaire **HAL**, est destinée au dépôt et à la diffusion de documents scientifiques de niveau recherche, publiés ou non, émanant des établissements d'enseignement et de recherche français ou étrangers, des laboratoires publics ou privés.

CONTROL OF THE EFFECTS OF REGULARIZATION ON VARIATIONAL OPTIC FLOW COMPUTATIONS

Z. BELHACHMI AND F. HECHT

ABSTRACT. We consider a variational model for the determination of the optic-flow in a general setting of non-smooth domains. This problem is ill-posed and its solution with PDE techniques includes a regularization procedure. The goal of this paper is to study a method to solve the optic flow problem and to control the effects of the regularization by allowing, locally and adaptively the choice of its parameters. The regularization in our approach is not controlled by a single parameter but by a function of the space variable. This results in a dynamical selection of the variational model which evolves with the variations of this function. Such method consists of new adaptive finite element discretization and an a posteriori strategy for the control of the regularization in order to achieve a trade-off between the data and the smoothness terms in the energy functional. We perform the convergence analysis and the a posteriori analysis, and we prove that the error indicators provide, as, a by-product, a confidence measure which shows the effects of regularization and serves to compute sparse solutions. We perform several numerical experiments, to show the efficiency and the reliability of the method in the computations of optic flow, with high accuracy and of low density.

1. INTRODUCTION

The computation of the displacement field between the subsequent frames of an image sequence is a classical problem in image processing . This displacement field is called the optic flow and is used in many applications (medical imaging, video processing, ...). Moreover, it belongs to a family of correspondence problems where one seeks a smooth mapping that maps the features in one image to another one. Its reliable computation constitutes a very challenging task in computer vision. Most of the methods to compute the optic flow are based on constancy assumptions on image features such as the gray levels, the brightness, ... In general, these assumptions are not sufficient for its determination and they allow only the estimation of the component normal to the edges of the image, this is the so-called aperture problem. It shows that the estimation of the optic flow is in fact an ill-posed

Date: October 22, 2009.

1991 Mathematics Subject Classification. 68U20, 47A52, 65N30.

Key words and phrases. computer vision, optic flow, regularization procedure, adaptive finite elements, confidence measure.

problem, we refer the reader to the reviews in [14, 36, 12] and the references therein.

The optic flow problems have received much attention in the image analysis community (see [13, 14, 15, 1, 2, 10, 3, 26, 29, 30, 32, 33, 36, 18] and the references therein). The variational methods are some of the most efficient approaches for solving such problems [14, 15, 3, 4, 25, 46, 37]. They consist in searching the solutions which are minimizers of suitable energy functionals. Their success is mainly due to the fact that the functional to minimize expresses the data constraints (constancy assumptions) and regularization terms (smoothness) to cope with the aperture problem and to recover a fully dense vector fields (defined in the entire domain). A major drawback of the variational methods is the reliability of the computed fields in all locations of the computational domain. While obtaining a dense vector fields is one of the advantages of such methods (no need for extra interpolation procedure), it is difficult to distinguish which parts of the estimated fields are due only to the filling-in effect of the regularization. This reliability is of great importance in many applications which use the optic flow techniques (for instance, in medical imaging, the optic flow allows to measure some physical quantities which are difficult to measure directly [38]).

To circumvent this difficulty, some confidence measures were proposed earlier in the literature to assess the reliability and to sparsify the estimated optic flow. The most widely used confidence measure is based on the magnitude of the image gradients [8, 39], but is not efficient (see the discussion in [13]). Recently, a local energy-based measure was introduced in [13], it seems to give better results than the previous one, but its derivation as well as its performances follow from heuristic considerations rather than by a well founded mathematical arguments. In particular, the main question on the reliability of the computations is clearly linked to a balance between the two competing terms of the energy (data constraints versus regularization) and not to the total energy. It turns out that building such confidence measures should be considered in a more general setting on how to control the regularization process (enforcing its effects only when and where it is necessary).

Most methods for the choice of the regularization parameters obey to the following paradigm [43, 21, 20]: Optimize, then discretize. Thus, the value of the parameter (usually a real number) is fixed thanks to some a priori estimates linking the noise magnitude and such value. This method is not robust with respect to the variations of the discretization parameters. In our case, to deal with a real valued function instead of a single parameter, we invert the paradigm: we discretize, then we optimize. To this end we use a sophisticated approach based on a posteriori estimates which allow to measure both the discretization error and the model error [5, 11].

In this paper, starting with a variational model we propose a finite element method for computing the optic flow which includes an implicit confidence

measure. Our strategy is based on locally adaptive choice of the regularization parameters which allows us to select and modify dynamically the initial model. The adaptation process is completely a posteriori and uses only the measure on the estimated optic flow, hence it differs from other approaches like the image-driven or the flow-driven regularization methods [1, 3] (where the models are given a priori) as well as from algorithmic approaches based on the multigrid method [31, 42] (where there is one single parameter of regularization and the number of cycles is fixed a priori). Moreover, even if the procedure of selecting locally the parameters is nonlinear (i.e. belongs to the nonlinear approximation theory), the variational model remains linear which is an advantage when comparing to flow-driven models [4].

This new approach of the control of the regularization increases the efficiency of most existing variational models currently used to solve problems of image analysis and of computer vision. In fact, it should be considered as a tool for selecting suited models by adjusting the influence of each term in the energy functional where various constraints of the considered problem are expressed. The selection is automatic and almost no hand tuning is required, which constitutes a promising method, in particular to design or to simplify some nonlinear models. Moreover, the method introduced in this paper, benefit from each improvement of the model (the energy functional) with respect to the data.

The adaptivity process which allows the local choice of the parameters is performed with a rigorous analysis of the residual error estimators. These are error indicators which are equivalent to the discretization error in an appropriate norm [44, 34, 9]. We use a modified energy norm depending on the regularization parameters used as scaling factors in the error indicators. Our goal is not only to provide an efficient method to solve optic flow problems but also to show how this error indicators constitute a natural confidence measure which yield a low density flow fields (i.e. achieve the goal of sparsification of the computed vector fields). In addition we use the error indicators to improve the computations results and to also build the “best” mesh for the optic flow. The method is, from this point of view, self contained and no extra confidence measures, nor sparsification process are needed. The method should also work with the finite difference method but our choice is related to the fact that the analysis and the adaptive process are more usual in the framework of finite element methods. In addition, this choice is enforced by the fact that well suited meshes for optic flow are usually unstructured. The cost of the interpolation on structured meshes where the images are given is low compared to cost of the computations in such grids (which are very large, particularly for high resolution images). Moreover, in many applications, the optic flow computations are used to estimate some physical data (wavefront, velocity of the blood in vessels or in the heart [38], ...). This data serve in other simulations in various finite element codes.

There exists a wide variety of variational models for optic flow determination [12, 45], linear, nonlinear, discontinuity-preserving, . . . In order to apply our program and to show the reliability of the method, we will consider a linear model introduced in [14, 15] called the CLG (Combined Local-Global) approach which is representative of variational linear optic flow methods. In a second part of this work (a forthcoming paper) we will present the method for some nonlinear models.

The paper is organized as follows: In Section 2 we state the variational optic flow model and we establish its principal properties. Section 3 is devoted to the finite element discretization and the well posedness. In section 4, we perform the a posteriori analysis and define the error indicators. In section 5, we discuss implementation issues. Numerical experiments are presented in Section 6. In appendix A, we establish the convergence of the discrete solutions and appendix B is devoted to the (rather) technical derivation of the a posteriori error estimates which justify mathematically our approach of the control of regularization.

2. VARIATIONAL OPTIC FLOW PROBLEM

Optic flow determination consists of finding a vector field (u_1, u_2) which describes the “motion” in a given sequence of an image. Given a domain $\Omega \in \mathbb{R}^2$ and a function $f : \Omega \times \mathbb{R} \rightarrow \mathbb{R}$ modeling a sequence of frames of an image, most models in optic flow problem are based on the constancy of the grey level of pixels which reads:

$$(1) \quad f(t, x_1, x_2) = f(t + 1, x_1 + u_1, x_2 + u_2)$$

For small displacements, if we assume $f \in C^1([0, +\infty[; \mathbb{R}^2)$, we are led to consider the following problem: find the displacement field $u_1(x_1, x_2)$, $u_2(x_1, x_2)$, such that

$$(2) \quad f_t + f_{x_1}u_1 + f_{x_2}u_2 = 0$$

The vector field (u_1, u_2) is called the optic flow.

Remark 2.1. *The equivalence of (1) and (3) is still valid if we assume $f \in C^0([0, +\infty[; L^1(\mathbb{R}^2))$ the derivatives in this case are to be understood in a weak sense.*

The principle of the variational approach is to determine $\mathbf{u} = (u_1, u_2)$ as the minimizer of a given energy functional. This functional is usually made of two parts: a data term which expresses the optic flow constraint (3) and a regularization term due to the fact that the first part does not yield a well posed problem. We refer the reader to [14, 15, 12] and the references therein for a complete review of the various models of functionals. In what follows, we will consider a linear model called the CLG approach [15].

We will denote by J_ρ the matrix $K_\rho * (\mathbf{grad} f \mathbf{grad} f^T)$, where we use the spatial gradient $(\frac{\partial}{\partial x_1}, \frac{\partial}{\partial x_2})^T$,

$$J_\rho = \begin{pmatrix} K_\rho * f_{x_1}^2 & K_\rho * f_{x_1} f_{x_2} \\ K_\rho * f_{x_1} f_{x_2} & K_\rho * f_{x_2}^2 \end{pmatrix},$$

and $K_\rho(x, y)$ is a Gaussian kernel with standard deviation ρ . Given a vector field \mathbf{v} , we denote by

$$\mathbf{grad}(\mathbf{v}) = \begin{pmatrix} \frac{\partial v_1}{\partial x_1} & \frac{\partial v_1}{\partial x_2} \\ \frac{\partial v_2}{\partial x_1} & \frac{\partial v_2}{\partial x_2} \end{pmatrix}.$$

We also denote for $\mathbf{v} = (v_1, v_2)$

$$\Delta \mathbf{v} = (\Delta v_1, \Delta v_2),$$

where Δv_1 is the Laplacian of the scalar function v_1 . We introduce the product

$$\mathbf{grad}(\mathbf{u}) : \mathbf{grad}(\mathbf{v}) = \sum_{i,j=1}^2 \frac{\partial u_i}{\partial x_j} \frac{\partial v_i}{\partial x_j}.$$

We set $\mathbf{f} = -K_\rho * (f_{x_1} f_t, f_{x_2} f_t)^T$, and $\mathbf{u} = (u_1, u_2)^T$, where f_{x_1} , f_{x_2} and f_t stand for the derivatives with respect to x_1 , x_2 and t respectively. For the sake of brevity we will denote by $\mathbf{u}^T J_\rho \mathbf{u}$, $J_\rho \mathbf{u}^2$ or $|J_\rho^{\frac{1}{2}} \mathbf{u}|^2$ the product

$$(J_\rho \mathbf{u}, \mathbf{u}),$$

where $(.,.)$ is the scalar product in \mathbb{R}^2 . In the pioneering work of Lucas and Kanade (1981) and Lucas (1984) proposed to solve (2) by minimizing the energy $K_\rho * (f_{x_1} u + f_{x_2} v + f_t)^2$. To obtain a dense flow estimates, Horn and Schunck (1981) have proposed to recover the functions $u(x_1, x_2, t)$ and $v(x_1, x_2, t)$ as minimizers of the global energy

$$\int_{\Omega} ((f_{x_1} u + f_{x_2} v + f_t)^2) + \alpha (|\mathbf{grad} u|^2 + |\mathbf{grad} v|^2) dx_1 dx_2$$

The CLG method proposed by Bruhn and Weickert (2005) is a combination of this two approaches. Our approach is a modification of this last model where we allow α to be a function of (x_1, x_2) .

In the rest of the paper we will denote by \mathbf{u} a solution to the equation

$$(3) \quad J_\rho \mathbf{u} = \mathbf{f}.$$

which could be interpreted as a minimizer of the functional

$$\int_{\Omega} |J_\rho^{\frac{1}{2}} \mathbf{u} - J_\rho^{-\frac{1}{2}} \mathbf{f}|^2 dx_1 dx_2.$$

In general, in the estimation of the optic flow problem, it is always assumed that the domain Ω is a smooth open set. This assumption becomes a restriction if one wants to deal with some altered images (satellite images, images with hidden part, ...) or for images with occlusions. We shall not

make such an assumption at least for the analysis of the continuous problem. The general functional setting of the optic flow consists in the following choice of the space

$$\mathcal{L}_\varrho^{1,2}(\Omega, \mathbb{R}^2) = \mathcal{L}_\varrho^{1,2}(\Omega) = \left\{ \mathbf{u} \in L_{\ell_{OC}}^2(\Omega); \mathbf{grad} \mathbf{u} \in L^2(\Omega), \int_{\Omega} |J_\varrho^{\frac{1}{2}} \mathbf{u}|^2 dx < \infty \right\},$$

where the gradient is taken in the sense of distributions. We define the equivalence relation:

$$\mathbf{u} \mathcal{R} \mathbf{v} \iff \int_{\Omega} |\mathbf{grad}(\mathbf{u} - \mathbf{v})|^2 dx + \int_{\Omega} J_\varrho(\mathbf{u} - \mathbf{v})^2 dx = 0.$$

The quotient space $(\mathcal{L}_\varrho^{1,2}(\Omega))/\mathcal{R} = L_\varrho^{1,2}(\Omega)$ is a Hilbert space for the scalar product

$$(\mathbf{u}, \mathbf{v})_\varrho = \int_{\Omega} \mathbf{grad} \mathbf{u} : \mathbf{grad} \mathbf{v} dx + \int_{\Omega} J_\varrho \mathbf{u} \cdot \mathbf{v} dx.$$

equipped with the norm

$$\|\mathbf{u}\|_{L_\varrho^{1,2}(\Omega)} = (\mathbf{u}, \mathbf{u})_\varrho^{\frac{1}{2}}$$

Note that if \mathbf{u}, \mathbf{v} belong to $\mathcal{L}_\varrho^{1,2}(\Omega)$ and $\mathbf{u} \mathcal{R} \mathbf{v}$ then, for any connected component $\omega \in \Omega$ such that $|\omega \cap \{J_\varrho > 0\}| = 0$, we have $\mathbf{u} - \mathbf{v} = \text{constant}$. If $|\omega \cap \{J_\varrho > 0\}| > 0$, then the constant is zero.

We consider the following energy functional associated with the optic flow recovery by variational methods

$$(4) \quad E(\mathbf{u}) = \int_{\Omega} (\mathbf{u}^T J_\varrho \mathbf{u} + \alpha(\mathbf{x}) |\mathbf{grad} \mathbf{u}|^2) dx - \int_{\Omega} \mathbf{f} \cdot \mathbf{u} dx,$$

where α is a given, scalar, piecewise constant function on Ω . Accordingly, we consider a disjoint partition into a finite number of subdomains Ω_ℓ , $1 \leq \ell \leq L$, such that the function α is equal to α_ℓ on each Ω_ℓ . We denote $\alpha_m = \min_{1 \leq \ell \leq L} \alpha_\ell$, respectively $\alpha_M = \max_{1 \leq \ell \leq L} \alpha_\ell$, and we assume that $\alpha_m > 0$.

In order to handle easily the degeneracy of J_ϱ (i.e. the compatibility condition on regions where J_ϱ is not definite) we will rewrite the datum \mathbf{f} , under the form $\mathbf{f} = J_\varrho \mathbf{h} + \mathbf{g}$, where \mathbf{h} is such that $(J_\varrho)^{\frac{1}{2}} \mathbf{h} \in L^2(\Omega)$, $\text{supp} \mathbf{g} \subset \Omega$ and $\int_{\omega} \mathbf{g} dx = 0$ for any connected component subset ω of Ω . Such a decomposition follows from the compatibility condition on \mathbf{f} to solve the Neumann problem

$$\begin{cases} \Delta \mathbf{u} + J_\varrho \mathbf{u} = \mathbf{f} & \text{in } \Omega, \\ \frac{\partial \mathbf{u}}{\partial n} = 0 & \text{on } \partial \Omega. \end{cases}$$

The variational optic flow problem consists of finding $\mathbf{u} \in L_\varrho^{1,2}(\Omega)$ such that

$$(5) \quad E(\mathbf{u}) = \inf_{\mathbf{v} \in L_\varrho^{1,2}(\Omega)} E(\mathbf{v}).$$

The existence of a weak solution \mathbf{u}_α of (5) follows from the Lax-Milgram Lemma. The only point to check is the continuity of the linear form $\mathbf{v} \mapsto \int_\Omega \mathbf{f} \cdot \mathbf{v} \, d\mathbf{x}$. We have

$$\begin{aligned} \left| \int_\Omega \mathbf{f} \cdot \mathbf{v} \, d\mathbf{x} \right| &\leq \int_\Omega |J_\varrho \mathbf{h} \cdot \mathbf{u}| \, d\mathbf{x} + \left| \int_\Omega \mathbf{g} \mathbf{u} \, d\mathbf{x} \right| \\ &\leq \left(\int_\Omega J_\varrho \mathbf{h}^2 \, d\mathbf{x} \right)^{\frac{1}{2}} \left(\int_\Omega J_\varrho \mathbf{u}^2 \, d\mathbf{x} \right)^{\frac{1}{2}} + C \left(\int_\omega |\mathbf{grad} \mathbf{u}|^2 \, d\mathbf{x} \right)^{\frac{1}{2}} \left(\int_\omega |\mathbf{g}|^2 \, d\mathbf{x} \right)^{\frac{1}{2}} \\ &\leq C \|\mathbf{u}\|_{L_\varrho^{1,2}(\Omega)}, \end{aligned}$$

where C is the Poincaré-Wirtinger inequality applied in $H^1(\omega, \mathbb{R}^2) \setminus \mathbb{R}^2$ and the smooth set ω is such that $\text{supp} \mathbf{g} \subset \omega \subset \Omega$.

Proposition 2.2. *Problem (5) admits a weak solution \mathbf{u}_α in $L_\varrho^{1,2}(\Omega)$.*

When Ω , \mathbf{f} , J_ϱ are sufficiently smooth, additional regularity could be proved for the solution \mathbf{u}_α . For instance, with Ω Lipschitz-continuous, $\mathbf{f} \in L^2(\Omega)$ and $J_\varrho \in L^{+\infty}(\Omega)$, the following regularity result holds [6, Proposition 2.5]

Proposition 2.3. *There exists a constant c only depending on the geometry of Ω , such that a weak solution \mathbf{u}_α of problem (5) belongs to $H^{s+1}(\Omega)$, for all real numbers $s < s_0$, where s_0 is given by*

$$s_0 = \min \left\{ \frac{1}{2}, c \left| \log \left(1 - \frac{\alpha_m}{\alpha_M} \right) \right| \right\}$$

The Euler-Lagrange equations are given by:

$$(6) \quad \begin{cases} \text{div}(\alpha(\mathbf{x}) \mathbf{grad} u_1) - (f_{x_1}^2 u_1 + f_{x_1} f_{x_2} u_2 + f_{x_1} f_t) = 0, & \text{in } \Omega, \\ \text{div}(\alpha(\mathbf{x}) \mathbf{grad} u_2) - (f_{x_1} f_{x_2} u_1 + f_{x_2}^2 u_2 + f_{x_2} f_t) = 0 & \text{in } \Omega, \\ \frac{\partial u_1}{\partial n} = \frac{\partial u_2}{\partial n} = 0, & \text{on } \partial\Omega, \end{cases}$$

Remark 2.4.

If Ω is not smooth, the Neumann condition on the boundary should be understood in the weak sense.

The weak formulation of (6) reads

$$(7) \quad \begin{cases} \text{Find } \mathbf{u} \in L_\varrho^{1,2}(\Omega), \text{ such that} \\ \int_\Omega \alpha(\mathbf{x}) \nabla \mathbf{u} : \nabla \mathbf{v} \, d\mathbf{x} + \int_\Omega J_\varrho \mathbf{u} \cdot \mathbf{v} \, d\mathbf{x} = \int_\Omega \mathbf{f} \cdot \mathbf{v} \, d\mathbf{x} \quad \forall \mathbf{v} \in L_\varrho^{1,2}(\Omega). \end{cases}$$

We introduce the notations: for $\mathbf{u}, \mathbf{v} \in L_\varrho^{1,2}(\Omega)$

$$(8) \quad \begin{aligned} a_\alpha(\mathbf{u}, \mathbf{v}) &= \int_\Omega \alpha(\mathbf{x}) \mathbf{grad} \mathbf{u} : \mathbf{grad} \mathbf{v} \, d\mathbf{x} + \int_\Omega J_\varrho \mathbf{u} \cdot \mathbf{v} \, d\mathbf{x}, \\ (\mathbf{f}, \mathbf{v}) &= \int_\Omega \mathbf{f} \cdot \mathbf{v} \, d\mathbf{x}, \end{aligned}$$

Thus, problem (7) consists of finding $\mathbf{u} \in L_\varrho^{1,2}(\Omega)$, such that

$$a_\alpha(\mathbf{u}, \mathbf{v}) = (\mathbf{f}, \mathbf{v}), \quad \forall \mathbf{v} \in L_\varrho^{1,2}(\Omega).$$

The equivalence of problem (7) and (6) follows by standard arguments.

2.1. Some useful inequalities. In order to obtain the error estimates with constants independent of α , we introduce the norm

$$\|\mathbf{u}\|_{\varrho,\alpha}^2 = \|\alpha^{\frac{1}{2}} \mathbf{grad} \mathbf{u}\|_{L^2(\Omega)}^2 + \|J_{\varrho}^{\frac{1}{2}} \mathbf{u}\|_{L^2(\Omega)}^2.$$

For a posteriori analysis purposes, we will assume that the matrix J_{ϱ} is definite a.e. This assumption is not restrictive in the computer vision problems because the data term is usually regularized.

In addition, to avoid inessential technicalities in the discretization we assume that Ω is Lipschitz-continuous domain. In this case the space $L_{\varrho}^{1,2}(\Omega) = H^1(\Omega)$ (see [23, Corollary 2.2]).

Remark 2.5. *Note that for nonsmooth domains, we may proceed by approximation in the spirit of [7]. The nonsmooth parts are approximated by smooth neighbourhoods on which the regularization parameter goes to zero.*

We prove now the following estimate

Proposition 2.6. *Let $\mathbf{u} \in H^1(\Omega)$ be a solution of problem (3). For $\alpha > 0$, the following estimates hold between \mathbf{u} and the solution \mathbf{u}_{α} of problem (7)*

$$(9) \quad \|\mathbf{u}_{\alpha}\|_{\varrho,\alpha} \leq C \|J_{\varrho}^{\frac{1}{2}} \mathbf{u}\|_{L^2(\Omega)},$$

and

$$(10) \quad \|\mathbf{u} - \mathbf{u}_{\alpha}\|_{\varrho,\alpha} \leq C \left(\frac{\alpha_M}{\alpha_m}\right)^{\frac{1}{2}} \|\alpha^{\frac{1}{2}} \mathbf{grad} \mathbf{u}_{\alpha}\|_{L^2(\Omega)},$$

with the constant C independent of α .

Proof. We have from (7) and (3)

$$\int_{\Omega} \alpha(\mathbf{x}) \mathbf{grad} \mathbf{u}_{\alpha} : \mathbf{grad} \mathbf{v} \, d\mathbf{x} + \int_{\Omega} J_{\varrho} \mathbf{u}_{\alpha} \cdot \mathbf{v} \, d\mathbf{x} = \int_{\Omega} J_{\varrho} \mathbf{u} \cdot \mathbf{v} \, d\mathbf{x} \quad \forall \mathbf{v} \in H^1(\Omega).$$

Choosing $\mathbf{v} = \mathbf{u}_{\alpha}$, we obtain

$$\begin{aligned} \int_{\Omega} \alpha(\mathbf{x}) |\mathbf{grad} \mathbf{u}_{\alpha}|^2 \, d\mathbf{x} &= \int_{\Omega} J_{\varrho} (\mathbf{u} - \mathbf{u}_{\alpha}) \mathbf{u}_{\alpha} \, d\mathbf{x}, \\ \int_{\Omega} \alpha(\mathbf{x}) |\mathbf{grad} \mathbf{u}_{\alpha}|^2 \, d\mathbf{x} + \int_{\Omega} J_{\varrho} \mathbf{u}_{\alpha}^2 \, d\mathbf{x} &= \int_{\Omega} J_{\varrho} \mathbf{u} \cdot \mathbf{u}_{\alpha} \, d\mathbf{x} \\ &\leq C \|J_{\varrho}^{\frac{1}{2}} \mathbf{u}\|_{L^2(\Omega)} \|J_{\varrho}^{\frac{1}{2}} \mathbf{u}_{\alpha}\|_{L^2(\Omega)}, \end{aligned}$$

which yields the inequality (9).

Again choosing $\mathbf{v} = \mathbf{u} - \mathbf{u}_{\alpha}$, we obtain

$$\begin{aligned} \int_{\Omega} \alpha(\mathbf{x}) \mathbf{grad} \mathbf{u}_{\alpha} \cdot \mathbf{grad} (\mathbf{u} - \mathbf{u}_{\alpha}) \, d\mathbf{x} &= \int_{\Omega} J_{\varrho} (\mathbf{u} - \mathbf{u}_{\alpha}) (\mathbf{u} - \mathbf{u}_{\alpha}) \, d\mathbf{x} \\ &= \int_{\Omega} J_{\varrho} (\mathbf{u} - \mathbf{u}_{\alpha})^2 \, d\mathbf{x}. \end{aligned}$$

Adding and subtracting the quantity $\int_{\Omega} \alpha(\mathbf{x}) \mathbf{grad} \mathbf{u} : \mathbf{grad} (\mathbf{u} - \mathbf{u}_{\alpha})$ and the Cauchy-Schwarz inequality yields, for any $\varepsilon > 0$

$$\begin{aligned} \int_{\Omega} \alpha(\mathbf{x}) \mathbf{grad} (\mathbf{u} - \mathbf{u}_{\alpha})^2 d\mathbf{x} + \int_{\Omega} J_{\varrho}(\mathbf{u} - \mathbf{u}_{\alpha})^2 d\mathbf{x} &= \int_{\Omega} \alpha(\mathbf{x}) \mathbf{grad} \mathbf{u} : \mathbf{grad} (\mathbf{u} - \mathbf{u}_{\alpha}) d\mathbf{x} \\ &\leq \alpha_M \|\mathbf{grad} \mathbf{u}\|_{L^2(\Omega)}^2 + \alpha_M^{1+2\varepsilon} \|\mathbf{grad} \mathbf{u}\|_{L^2(\Omega)}^2 \\ &\quad + \frac{\alpha_M}{\alpha_m} \alpha_M^{-2\varepsilon} \|\alpha^{\frac{1}{2}} \mathbf{grad} \mathbf{u}_{\alpha}\|_{L^2(\Omega)}^2. \end{aligned}$$

which yields (10) □

Note that we are only interested here in the behaviour of (\mathbf{u}_{α}) as the ratio $\frac{\alpha_M}{\alpha_m}$ is large because we intend to adapt locally the choice of the regularization parameters α . The bound (10) will be used to complete the error indicator to obtain a confidence measure allowing as well for a good choice of α , and to build an adapted mesh for the optic flow.

It follows from proposition 2.3 that \mathbf{u}_{α} is $H^1(\Omega)$. While, there is a priori no reason that \mathbf{u} a solution of (3) belongs to $H^1(\Omega)$. A reasonable assumption on the regularity for a solution of (3) is to be in the space BV , but for the discretization purpose we prefer to work in the Hilbertian framework. Therefore an appropriate choice is the space

$$X = \{ \mathbf{v} \in L^2(\Omega); \mathbf{v}|_{\Omega_{\ell}} \in H^1(\Omega_{\ell}), 1 \leq \ell \leq L \},$$

which allows for jumps across the boundaries of the subdomains Ω_{ℓ} . The results of proposition 2.6 extend to this case by replacing the norm with the broken one

$$\|\mathbf{u}\|_X = \left(\sum_{\ell=1}^L \alpha_{\ell}^{\frac{1}{2}} \|\mathbf{grad} \mathbf{u}\|_{L^2(\Omega_{\ell})}^2 + \|J_{\varrho}^{\frac{1}{2}} \mathbf{u}\|_{L^2(\Omega)}^2 \right)^{\frac{1}{2}}.$$

For simplicity we will assume that we have a solution \mathbf{u} in $H^1(\Omega)$.

3. DISCRETE PROBLEM

We assume that the domain Ω is polygonal. We consider a regular family of triangulations $(\mathcal{T}_h)_h$ made of elements which are triangles (or quadrilaterals) with a maximum size h , satisfying the usual admissibility assumptions, i.e. the intersection of two different elements is either empty, a vertex, or a whole edge. The ratio of the diameter of any element $T \in \mathcal{T}_h$ to the diameter of its largest inscribed ball is bounded by a constant σ independent of T and h .

We introduce the following discrete space: for $h > 0$

$$\mathbf{V}_h = \{ \mathbf{v}_h \in C(\overline{\Omega}), \mathbf{v}_h|_T \in P_1(T)^2 \}.$$

We denote by $J_{\varrho,h}$ a finite element approximation of the matrix J_{ϱ} obtained as follows: for any $K \in \mathcal{T}_h$ we denote by $J_{\varrho,h,K}$ the matrix where the coefficients

$$(J_{\varrho,h,K})_{i,j} = \frac{1}{|K|} \int_K (J_{\varrho})_{i,j} d\mathbf{x}, \quad 1 \leq i, j \leq 2,$$

are the mean values of the coefficients of J_{ϱ} on K . The matrix $J_{\varrho,h}$ is the piecewise constant matrix which takes the value $J_{\varrho,h,K}$ on the element K .

We denote by $a_{\alpha,h}$, the bilinear form a_{α} , where J_{ϱ} is replaced by $J_{\varrho,h}$. The discrete problem reads

$$(11) \quad \begin{cases} \text{find } \mathbf{u}_{\alpha,h} \in \mathbf{V}_h, \text{ such that} \\ a_{\alpha,h}(\mathbf{u}_{\alpha,h}, \mathbf{v}_h) = (\mathbf{f}, \mathbf{v}_h), \quad \forall \mathbf{v}_h \in \mathbf{V}_h, \end{cases}$$

Under the assumption of the definiteness of J_{ϱ} , the ellipticity of the bilinear form $a(\cdot, \cdot)_{\alpha,h}$ holds. Applying the Lax-Milgram Lemma, we have

Proposition 3.1. *For any $\alpha > 0$ there exists a unique solution $\mathbf{u}_{\alpha,h}$ of the discrete problem (11).*

4. THE CONFIDENCE MEASURE BY RESIDUAL ERROR INDICATOR

For the a posteriori error estimates we assume that $\mathbf{f} \in L^2(\Omega)^2$ and we fix \mathbf{f}_h a finite element approximation of it associated with \mathcal{T}_h . We also fix a finite element approximation $\tilde{J}_{\varrho,h}$ of J_{ϱ} . For $K \in \mathcal{T}_h$, we denote by \mathcal{E}_K the set of its edges not contained in the boundary $\partial\Omega$. The union of all \mathcal{E}_K , $K \in \mathcal{T}_h$ is denoted by \mathcal{E}_h . With each edge $e \in \mathcal{E}_h$, we associate a unit vector \mathbf{n}_e normal to e and we denote by $[\varphi]_e$ the jump of the piecewise continuous (vector valued) function φ across e in the direction \mathbf{n}_e . For each $K \in \mathcal{T}_h$ we denote by h_K the diameter of K and we denote by h_e the diameter of e , $e \in \mathcal{E}_K$.

We define the residual error indicators [44] as follows: For each element $K \in \mathcal{T}_h$, we set

$$(12) \quad \eta_K = \alpha_K^{-\frac{1}{2}} h_K \|\mathbf{f}_h + \alpha_K \Delta(\mathbf{u}_{\alpha,h}) + \tilde{J}_{\varrho,h} \mathbf{u}_{\alpha,h}\|_{L^2(K)^2} + \frac{1}{2} \sum_{e \in \mathcal{E}_K} \alpha_e^{-\frac{1}{2}} h_e^{\frac{1}{2}} \|[\alpha \mathbf{grad}(\mathbf{u}_{\alpha,h}) \mathbf{n}_e]_e\|_{L^2(e)^2},$$

where $\alpha_e = \max(\alpha_{K_1}, \alpha_{K_2})$, K_1 and K_2 being the two elements adjacent to e .

Theorem 4.1. *There exists a constant C which is independent of h and α such that the following estimate holds*

$$(13) \quad \|\mathbf{u}_{\alpha} - \mathbf{u}_{\alpha,h}\|_{\varrho,\alpha} \leq C \left(1 + \frac{\alpha_M}{\alpha_m}\right)^{\frac{1}{2}} \left(\sum_{K \in \mathcal{T}_h} \eta_K^2 + h_K^2 \alpha_K^{-1} \|\mathbf{f} - \mathbf{f}_h\|_{L^2(K)}^2\right)^{\frac{1}{2}}.$$

Combining (13) and (10) we obtain

Corollary 4.2. *Let \mathbf{u} be a solution of problem (3). There exists a constant C which is independent of h and α such that the following estimate holds*

$$(14) \quad \|\mathbf{u} - \mathbf{u}_{\alpha,h}\|_{\varrho,\alpha} \leq C \left(1 + \frac{\alpha_M}{\alpha_m}\right)^{\frac{1}{2}} \left(\sum_{K \in \mathcal{T}_h} \eta_K^2 + h_K^2 \alpha_K^{-1} \|\mathbf{f} - \mathbf{f}_h\|_{L^2(K)}^2 + \alpha_K \|\mathbf{grad} \mathbf{u}_\alpha\|_{L^2(K)}^2 \right)^{\frac{1}{2}}.$$

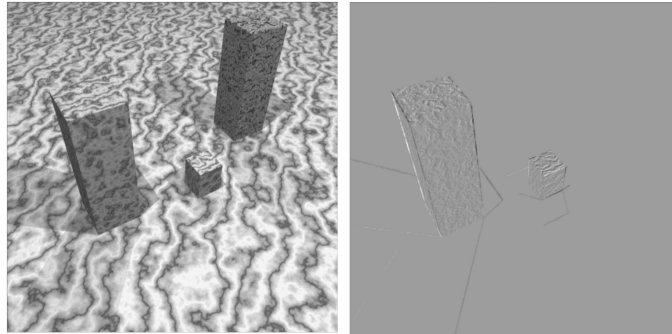
Note that in the last term in (14) the continuous solution \mathbf{u}_α appears. thus the inequality is not fully an posteriori estimate. However, the local finite element error, which is high order (for piecewise affine element $O(h_K^2)$), allows us to replace in this term \mathbf{u}_α by its discrete counterpart $\mathbf{u}_{\alpha,h}$. In this case, the meaning of inequality (14) is the following: For each element $K \in \mathcal{T}_h$, we have a new error indicator

$$(15) \quad \tilde{\eta}_K = \eta_K + \alpha_K^{\frac{1}{2}} \|\mathbf{grad} \mathbf{u}_{\alpha,h}\|_{L^2(K)}$$

This indicator gives an error map which shows both the finite elements error and the error on the model. Thus we have an upper bound for the error between an $H^1(\Omega)$ solution of the initial problem (without regularization) and the discrete regularized solution. This upper bound provides a natural confidence measure, completely computable from the discrete solution, and allows for an optimal locally adaptive choice of α . Figure 2(a)-Figure 2(f) show the maps given by the error indicator η_K and $\alpha_K |\mathbf{grad} \mathbf{u}_{\alpha,h}|_{L^2(K)}^2$, as well as the angular error (17) (see the next section for the definition) in the first and the final iterations. The graphs show the isovalues (Large values are in dark color and the low values in clear color).

In case we use an affine finite element discretization as in this paper, the new term $\alpha_K^{\frac{1}{2}} \|\mathbf{grad} \mathbf{u}_{\alpha,h}\|_{L^2(K)}$ behaves like $\alpha_K^{\frac{1}{2}} h_K$, is of the same order, and is consistent with η_K as shown by the figures.

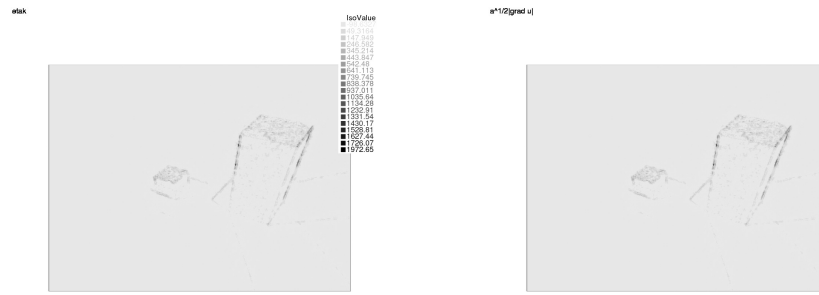
For the angular error, since we decrease the values of α near the edges of the optic flow (to have less regularization), this increases its maximum values (localized on some small parts of the edges) but the average is decreasing (see the convergence curve Figure 10(a)).



(a) frame 151 of the new marble sequence

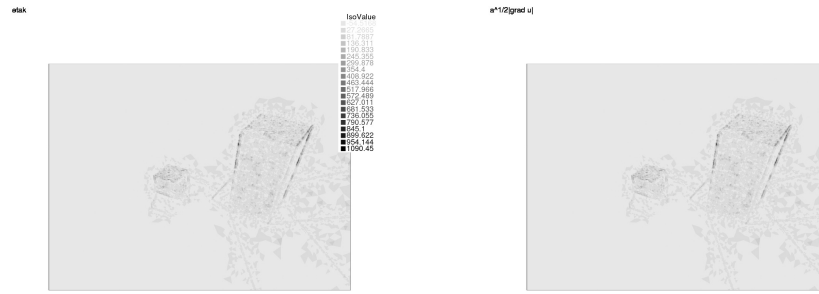
(b) time derivative f1-f2

FIGURE 1. New marble sequence (data)



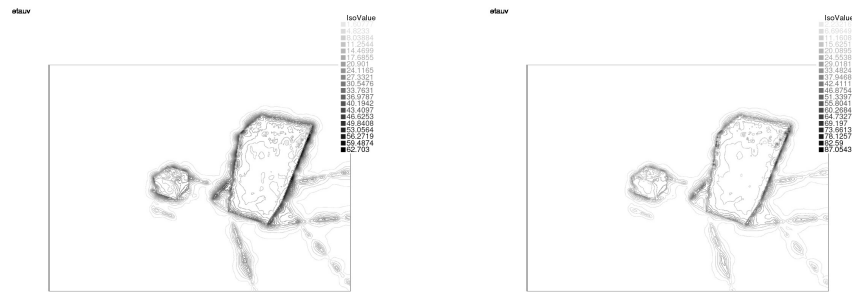
(a) error indicator η_K at iterarion k=1

(b) error indicator $\tilde{\eta}_K - \eta_K$ at k=1



(c) error indicator η_K at k=18

(d) error indicator $\tilde{\eta}_K - \eta_K$, k=18



(e) the angular error at iterarion k=1

(f) the angular error k=18

FIGURE 2. New marble sequence

5. ADAPTIVE STRATEGY AND NUMERICAL EXPERIMENTS

All numerical experiments are carried out with FreeFem++ [24]. We did not perform any optimization of the CPU time in our computations. The computational efficiency is no problem for variational methods when state-of-the-art numerical methods are used (see [45]). The computation of the matrix $J_{\rho,h}$ is performed by using a P1 approximation with mass lumping which is known to be a stable and accurate method. We do not smooth much the initial image and its gradient because we are mainly interested at this stage to show how our strategy works. Further efforts and improvements in the implementation issues are to be considered later.

5.1. Adaptive strategy. The adaptive process developed in this paper differs from the usual mesh adaptation because the geometric domain is given as the domain of definition of the image and it is usually not useful to refine it more. The adapted mesh for the optic flow computations is obtained by formally coarsening the initial grid. The algorithm reads:

- (1) We start with the cartesian grid \mathcal{T}_h^0 corresponding to the image.
- (2) **adaptivity steps**
 - Compute $\mathbf{u}_{\alpha_0,h}$ on \mathcal{T}_h^0 with $\alpha = \alpha_0$ a large constant.
 - We build an adapted isotropic mesh \mathcal{T}_h^1 (in the sense of the finite element method, i.e. with respect to the parameter h) with the metric error indicator which is well suited for the flow $\mathbf{u}_{\alpha_0,h}$.
 - We perform the local adaptive choice of $\alpha(x)$ on \mathcal{T}_h^1 and obtain a new function $\alpha_1(x)$.
- (3) Go to step 2 and compute $\mathbf{u}_{\alpha_1,h}$ on \mathcal{T}_h^1

Let us give more details on the implementation of this algorithm. On the triangulation $\mathcal{T}_{h,n}$, we compute the solution $\mathbf{u}_{\alpha_n,h}$ of problem (11), the corresponding error indicators as defined in (12) In addition to the standard information on the error distribution on the computations of $\mathbf{u}_{\alpha_n,h}$, the error indicators act as a confidence measure locating regions of large errors on the gradients (edges).

Note that all meshes \mathcal{T}_h^n are obtained by mesh adaptivity such that the minimal mesh sizes are greater than 1 which is the size of a pixel.

The principle of the adaptive regularization process is to decrease the values of α in regions where the error indicator is large (edges) and to increase the values in the complementary regions. However, for stability reasons we start with a relatively high initial guess and during the adaptive process α decreases following the formula:: for each triangle K

$$(16) \quad \alpha_K^{n+1} = \max\left(\frac{\alpha_K^n}{1 + \kappa * \left(\left(\frac{\eta_K}{\|\eta\|_\infty}\right) - 0.1\right)^+}, \alpha_{trh}\right).$$

where α_{trh} is a treshold and κ is a coefficient chosen for the control the rate of decreasing of α , $(u)^+ = \max(u, 0)$, and $\|\eta\|_\infty = \max_K(\eta_K)$.

This formula could be explained as follows: first we normalize η_K ($\in (0, 1)$) and if it is greater to 10% then we decrease the value of α . The value 10% as well as the choice of κ are chosen experimentally (Typical κ are 5 or 10 in our examples) .

- Remark 5.1.** i) *In these formulas we make the choice of taking α , more or less, constant in regions where the flow is smooth and the error indicator is small.*
 ii) *When some a priori information on regions of uncertainties or damaged regions in the image are available, we may keep the value of α very small (in these regions) which allows us to approximate correctly the Neumann boundary conditions in such nonsmooth situations.*

The adaptive strategy is performed either for a fixed (small) number of iterations or until the angular error increases. We note that the convergence is fast which is expected from the fact that the mesh T_h^1 corresponds, already, to sparse optic flow with a reasonably small angular error.

Thus, the adaptivity gives rise to sparse optic flow and an active control of the regularization effects. The algorithm is efficient in the sense that we obtain the regularized optic flow with a few elements (computational efficiency) and a map (the graph of $\alpha(x)$) which constitute a natural confidence measure.

In the following examples we give an illustration of our adaptive approach to the optic flow determination.

5.2. Example of the new marble. As a first example we consider the New Marble (introduced in the previous section), which is taken from <http://i21www.ira.uk.de/image/sequences>. We have sequences of 512 x 384 color images (polyhedral scene with two moving marbled blocks and stationary camera), Figure 1(a)-Figure 1(b). We give the evolution of the meshes for some iterations. It can be noted that the meshes are progressively sparsified (see also the tables given at the end of the section). Of course we do not plot the mesh T_h^0 which is the regular grid corresponding to the image (with 196608 elements). We also give the distribution of $\log(\alpha)$ and the modulus of the optic flow, Figure 3(a)-Figure 3(d) and Figure 4(a)-Figure 4(d) (for $\log(\alpha)$, large values are represented by dark colors and low values are in clear colors, for the modulus of the optic flow, the color map is inverted -for a technical reason in the software-).

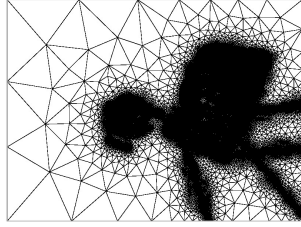
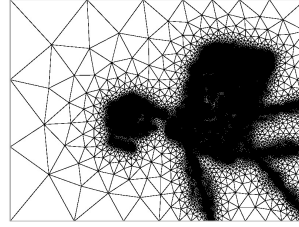
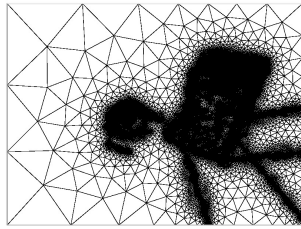
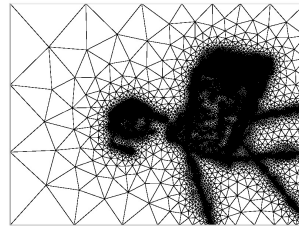
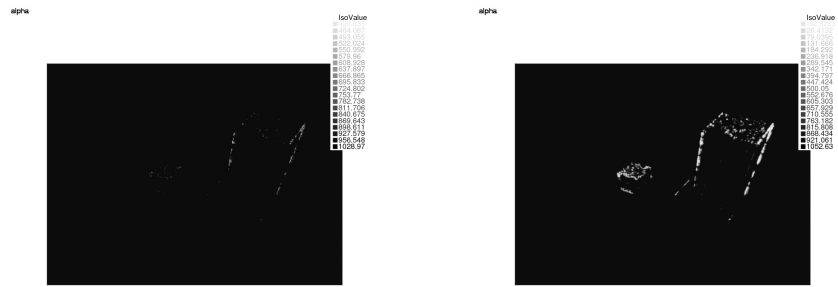
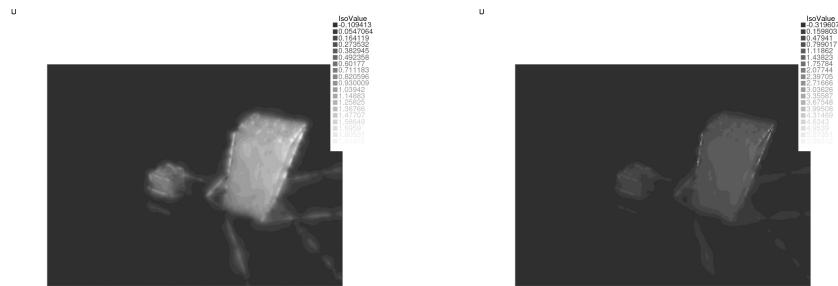
(a) the mesh at iteration $k=1$ (b) the mesh at iteration $k=6$ (c) the mesh at iteration $k=12$ (d) the mesh at (final) iteration $k=19$

FIGURE 3. Evolution of the meshes (New marble sequence)



(a) The distribution of $\log(\alpha)$, $k=1$

(b) The distribution of $\log(\alpha)$, $k=19$



(c) The modulus of optic flow, $k=1$

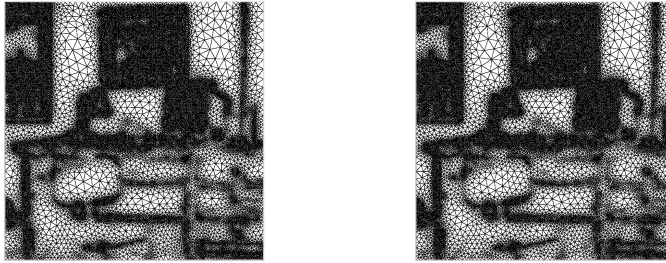
(d) The modulus of optic flow, $k=19$

FIGURE 4. New marble.

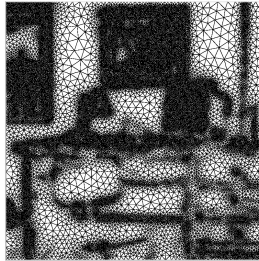


(a) frame 1 of the office sequences (b) time derivative f1-f2 sequences

FIGURE 5. Office sequence (data)



(a) the adapted mesh at iteration k=1 (b) the adapted mesh at iteration k=2



(c) the adapted mesh at iteration k=3

FIGURE 6. Meshes for the office sequence

5.3. Example of the office sequence. In this example of the office sequence taken from <http://www.cs.otago.ac.nz/research/vision>. We have 20 frames of color images. We represent the same quantities as in the previous example for the initial and the final iterations. The results are plotted in Figure 6(a)-Figure 6(c) and Figure 7(a)-Figure 7(d)

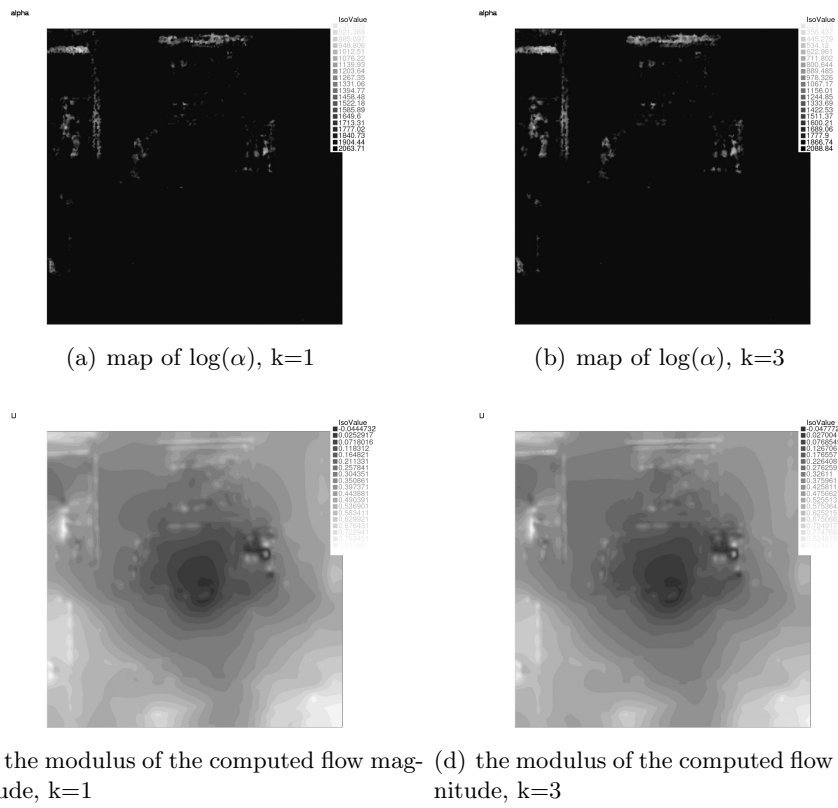


FIGURE 7. Office sequence

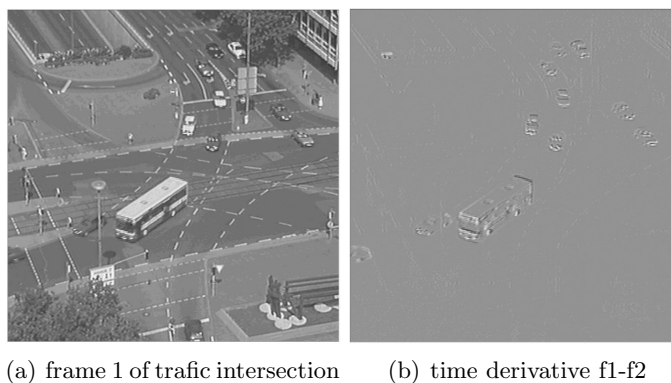
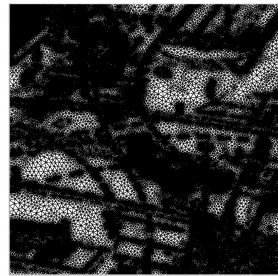
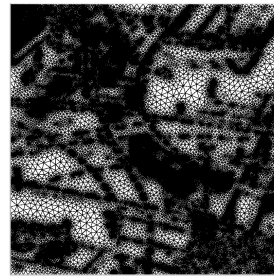


FIGURE 8. Traffic sequence (Data)

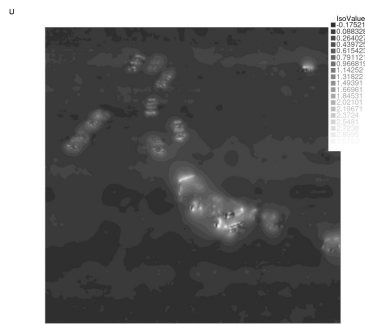
5.4. Example of traffic intersection. In this last example we have a traffic intersection sequence recorded at the Ettlinger-Tor in Karlsruhe by a stationary camera: 512×512 grayvalue images (<http://i21www.ira.uk.de/image/-sequences>). Figure 8(a)-Figure 8(b). We only give the meshes and the modulus of the optic flow in the case of this complex motion in Figure 9(a)-Figure 9(d).



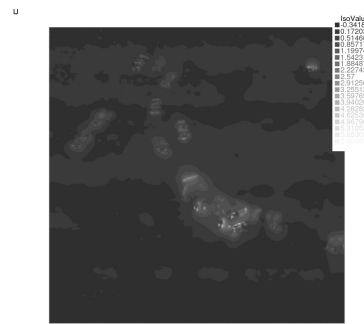
(a) mesh at iteration $k=1$



(b) mesh at iteration $k=9$



(c) The modulus of the optic flow, $k=1$



(d) The modulus of the optic flow, $k=9$

FIGURE 9. Traffic sequence

In order to show how our algorithm works quantitatively, we give the tables of the number of elements at each iteration (tables below) in the examples new marble and the office. We give also in tables 1 and 2, the evolution of the angular error and the number of degrees of freedom during the iterations. All these results show that the number of elements decreases very quickly at the first iteration, then more slowly to improve the sparsification by adjusting α . The values of α decrease, only on (some parts of) edges of the computed optic flow. Hence allowing to obtain sharp edges and less regularization (smoothing) at these locations. The coarsening of the mesh occurs far from these locations where increasing the regularization effects, allows for the reduction of the degrees of freedom.

Recall that the angular error is given by the formula

$$(17) \quad \arccos \frac{u_c u_e + v_c v_e + 1}{\sqrt{(u_c^2 + v_c^2 + 1)(u_e^2 + v_e^2 + 1)}},$$

where (u_c, v_c) denotes the correct flow and (u_e, v_e) the estimated one.

We end this section by giving the average of the angular error AAE, the number of degrees of freedom and the standard deviation at each iteration in the examples of new marble and of the office sequences. It can be seen from the tables 1 and 2, that the error decreases almost during the adaptivity process as well as the number of degrees of freedom (implying the sparsification of the flow). The angular error at iteration 0 is only depending on the initial guess α_0 , so it has already a reasonable value if α_0 is well chosen. In the algorithm, we start with large α_0 (a lot of smoothing) and we decrease the amount of the regularization in regions where it is necessary. We reach the convergence of the algorithm in a few iterations. The angular error and the density of the flow, decrease jointly. We stop when the AAE, start to increase. This is shown in two results of convergence in Figure 10(a) for the angular error and Figure 10(b) for the number of degrees of freedom. These curves show how the algorithm works: after the first iteration we obtain a “good” mesh for the optic flow, so that the discretization error is already small, the remaining iterations consists in adapting the values of α at edges.

Finally, we add two results of convergence in Figure 10(a) for the angular error and Figure 10(b) for the number of degrees of freedom. These curves show how the algorithm works: after the first iteration we obtain a “good” mesh for the optic flow, so that the discretization error is already small, the remaining iterations consists in adapting the values of α at edges.

iteration	nb vertices	AAE	Standard deviation
0	196608	2.9188	6.43791
1	33410	2.91485	6.43287
2	31687	2.90543	6.41461
3	31199	2.90111	6.40858
4	31074	2.89477	6.3947
5	30976	2.89341	6.39048
6	30906	2.89302	6.39158
7	30900	2.88896	6.38469
8	30599	2.88565	6.38095
9	30571	2.88393	6.37929
10	30535	2.88014	6.37313
11	30461	2.87483	6.36764
12	29308	2.87271	6.36766
13	28358	2.8673	6.36289
14	28044	2.86223	6.36047
15	26881	2.86009	6.36584
16	25723	2.85655	6.37016
17	24928	2.85721	6.37458
18	23073	2.85383	6.37729
19	21902	2.85606	6.38546

TABLE 1. Angular error for the marble example ($\alpha_0 = 1000$)

iteration	nb vertices	AAE	Standard deviation
0	40000	7.41066	4.65239
1	19424	7.43836	4.6439
2	19379	7.45966	4.63404

TABLE 2. Angular error for the office example ($\alpha_0 = 2000$)

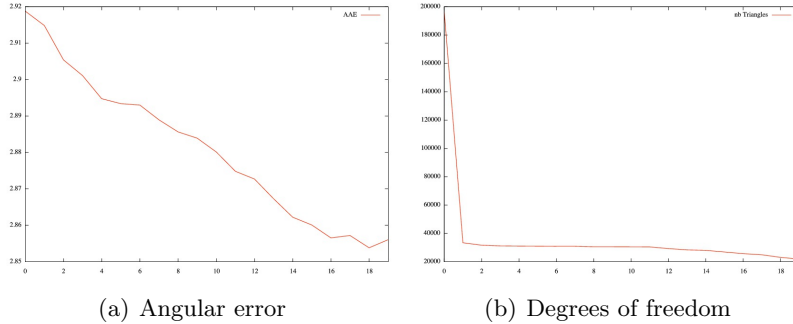


FIGURE 10. Convergence results

6. CONCLUSIONS

We have proposed a new a posteriori strategy to control the effects of the regularization of ill-posed problems. It allows locally adaptive choice of the regularization parameters which is very promising for an efficient and automatic model selection. This approach applied to the optical flow estimation yields a low density field with good accuracy. The method is not a new model to compute the optic flow but should be seen as a tool to enhance the existing variational methods [45], allowing the dynamical selection of the model by adaptive changes in the energy functional. This approach is at the beginning, and many improvements should be worked out, for example to go towards real time computations, It should also be used with the more sophisticated models proposed currently in the literature for its full validation. We restricted ourselves to simple models in order to focus on the main ideas but much remains to be done for improvements. Finally note that in the image analysis problems, nonlinear regularization methods, such as BV -regularization, are more suitable to preserve edges. The use of our method in this last case is under consideration. We believe, that the combination of our method and existing regularization techniques, image-driven, flow-driven, and multigrid methods, is a challenging and promising direction of research to solve ill-posed problems.

APPENDIX A

In this appendix we prove the following convergence result

Theorem 6.1. *Assume that the solution \mathbf{u}_α of (7) belongs to $(\bigcup_{\ell=1}^L H^2(\Omega_\ell)) \cap H^1(\Omega)$. There exists a constant C , which depends neither on h nor on α , such the following estimate holds*

$$(18) \quad \|\mathbf{u}_\alpha - \mathbf{u}_{\alpha,h}\|_{\varrho,\alpha} \leq C \sum_{\ell=1}^L \sqrt{\alpha_\ell} h_\ell \|\mathbf{u}_\alpha\|_{H^2(\Omega_\ell)}$$

The starting point for the convergence analysis is the abstract error estimate which follows from the so called Cea's lemma [17]

$$(19) \quad \|\mathbf{u}_\alpha - \mathbf{u}_{\alpha,h}\|_{\varrho,\alpha} \leq C \left(\inf_{\mathbf{v}_h \in \mathbf{V}_h} \|\mathbf{u}_\alpha - \mathbf{v}_h\|_\alpha + \sup_{\mathbf{w}_h \in \mathbf{V}_h} \frac{(a_\alpha - a_{\alpha,h})(\mathbf{v}_h, \mathbf{w}_h)}{\|\mathbf{w}_h\|_{\varrho,\alpha}} \right)$$

We denote by Π_h^α the orthogonal projection from $H^1(\Omega)$ onto \mathbf{V}_h for the norm $\|\cdot\|_{\varrho,\alpha}$.

Proposition 6.2. *For any real number s , with $1 \leq s \leq 2$, there exists a constant C , which depends neither on h nor on α , such that for any $\mathbf{v} \in (\bigcup_{\ell=1}^L H^s(\Omega_\ell)) \cap H^1(\Omega)$, the following estimate holds*

$$(20) \quad \|\mathbf{v} - \Pi_h^\alpha \mathbf{v}\|_{\varrho,\alpha} \leq C \sum_{\ell=1}^L \sqrt{\alpha_\ell} h_\ell^{(s-1)} \|\mathbf{grad} \mathbf{v}\|_{H^{s-1}(\Omega_\ell)}.$$

Proof. Let us start with $s = 2$, then

$$\|\mathbf{v} - \Pi_h^\alpha \mathbf{v}\|_{\varrho,\alpha} \leq \|\mathbf{v} - I_h \mathbf{v}\|_{\varrho,\alpha},$$

where I_h denotes the Lagrange interpolation operator at the vertices of the elements in \mathcal{T}_h . The standard estimate [17, Thm 16.1], for each $1 \leq \ell \leq L$

$$|\mathbf{v} - I_h \mathbf{v}|_{H^1(\Omega_\ell)} \leq c h_\ell \|\mathbf{grad} \mathbf{v}\|_{H^1(\Omega_\ell)},$$

yields the result. Next for $s = 1$ the inequality (20) follows from the definition of Π_h^α . A standard Hilbertian interpolation argument yields the general result. \square

In order to estimate the second term of the error, we note that

$$\begin{aligned} (a_\alpha - a_{\alpha,h})(\mathbf{v}_h, \mathbf{w}_h) &= \sum_{K \in \mathcal{T}_h} \left| \int_K (J_\varrho - J_{\varrho,h}) \mathbf{v}_h \cdot \mathbf{w}_h \, d\mathbf{x} \right| \\ &\leq \sum_{K \in \mathcal{T}_h} |J_\varrho - J_{\varrho,h}|_{L^\infty(K)} \|\mathbf{v}_h\|_{L^2(K)} \|\mathbf{w}_h\|_{L^2(K)} \\ &\leq \sum_{K \in \mathcal{T}_h} \lambda_{\min(J_\varrho)}^{-\frac{1}{2}} |J_\varrho - J_{\varrho,h}|_{L^\infty(K)} \|J_\varrho^{\frac{1}{2}} \mathbf{v}_h\|_{L^2(K)} \|J_\varrho^{\frac{1}{2}} \mathbf{w}_h\|_{L^2(K)}. \end{aligned}$$

Using the inequality [19, Thm 7.1]: for all $v \in W^{1,\infty}(K)$,

$$\inf_{q \in P_0} |v - q|_{L^\infty(K)} \leq c h_K |v|_{W^{1,\infty}(K)},$$

we obtain

$$(21) \quad |(a_\alpha - a_{\alpha,h})(\mathbf{v}_h, \mathbf{w}_h)| \leq C \lambda_{\min(J_\varrho)}^{-\frac{1}{2}} |J_\varrho|_{W^{1,\infty}(\Omega)} h \|\mathbf{v}_h\|_{\varrho,\alpha} \|\mathbf{w}_h\|_{\varrho,\alpha}$$

Assembling these estimates yields (18)

APPENDIX B

In this appendix we perform the a posteriori analysis which is the mathematical justification of our adaptive strategy. This analysis consists in proving that the error indicators introduced in (12) and (15) are equivalent locally to the discretization error and the model error. The proofs are rather technical because there are several nonconformities, we refer the unfamiliar readers to the monograph [44] for a complete and comprehensive introduction to the fields of a posteriori analysis.

6.1. An upper bound for the error. From the ellipticity of $a_\alpha(\cdot, \cdot)$ and $\mathbf{V}_h \subset H^1(\Omega)$, we have

$$\|\mathbf{u}_\alpha - \mathbf{u}_{\alpha,h}\|_{\varrho,\alpha}^2 = a_\alpha(\mathbf{u}_\alpha - \mathbf{u}_{\alpha,h}, \mathbf{u}_\alpha - \mathbf{u}_{\alpha,h}).$$

Choosing $\mathbf{v} \in \mathbf{V}_h$ in (8) and subtracting from (11), we obtain

$$(22) \quad ea_\alpha(\mathbf{u}_\alpha, \mathbf{v}) = a_{\alpha,h}(\mathbf{u}_{\alpha,h}, \mathbf{v}) \quad \forall \mathbf{v} \in \mathbf{V}_h.$$

We set $\mathbf{v} = J_\varrho^{-\frac{1}{2}}(\mathbf{u}_\alpha - \mathbf{u}_{\alpha,h})$ and we will denote by \mathbf{v}_h a given approximation of $J_\varrho^{\frac{1}{2}}\mathbf{v}$ in \mathbf{V}_h . The approximation \mathbf{v}_h will be defined later. Thus, we have

$$\begin{aligned} \|\mathbf{u}_\alpha - \mathbf{u}_{\alpha,h}\|_{\varrho,\alpha} &= a_\alpha(\mathbf{u}_\alpha - \mathbf{u}_{\alpha,h}, J_\varrho^{\frac{1}{2}}\mathbf{v} - \mathbf{v}_h) + a_\alpha(\mathbf{v}_h, \mathbf{u}_\alpha - \mathbf{u}_{\alpha,h}) \\ &= a_\alpha(\mathbf{u}_\alpha - \mathbf{u}_{\alpha,h}, J_\varrho^{\frac{1}{2}}\mathbf{v} - \mathbf{v}_h) + (a_{\alpha,h} - a_\alpha)(\mathbf{v}_h, \mathbf{u}_{\alpha,h}) \end{aligned}$$

We integrate by parts the first term on the right-hand side in each element $K \in T_h$. This leads to

$$\begin{aligned}
 a_\alpha(\mathbf{u} - \mathbf{u}_{\alpha,h}, J_\varrho^{\frac{1}{2}} \mathbf{v} - \mathbf{v}_h) &= \sum_{K \in T_h} \alpha_K \int_K \mathbf{grad}(\mathbf{u}_\alpha - \mathbf{u}_{\alpha,h}) : \mathbf{grad}(J_\varrho^{\frac{1}{2}} \mathbf{v} - \mathbf{v}_h) + \\
 &\quad \int_K J_\varrho(\mathbf{u}_\alpha - \mathbf{u}_{\alpha,h}) \cdot (J_\varrho^{\frac{1}{2}} \mathbf{v} - \mathbf{v}_h) \, d\mathbf{x} \\
 &= \sum_{K \in T_h} \alpha_K \int_K (-\Delta \mathbf{u}_\alpha + \Delta \mathbf{u}_{\alpha,h}) \cdot (J_\varrho^{\frac{1}{2}} \mathbf{v} - \mathbf{v}_h) \, d\mathbf{x} \\
 &\quad + \int_{\partial K} \alpha_K \mathbf{grad}(\mathbf{u}_\alpha - \mathbf{u}_{\alpha,h}) \mathbf{n} \cdot (J_\varrho^{\frac{1}{2}} \mathbf{v} - \mathbf{v}_h) \, d\sigma + \int_K J_\varrho(\mathbf{u}_\alpha - \mathbf{u}_{\alpha,h}) \cdot (J_\varrho^{\frac{1}{2}} \mathbf{v} - \mathbf{v}_h) \, d\mathbf{x} \\
 &= \sum_{K \in T_h} \int_K (\mathbf{f} + \alpha_K \Delta \mathbf{u}_{\alpha,h} - J_\varrho \mathbf{u}_{\alpha,h}) \cdot (J_\varrho^{\frac{1}{2}} \mathbf{v} - \mathbf{v}_h) \, d\mathbf{x} \\
 &\quad + \frac{1}{2} \sum_{e \in \mathcal{E}_K} \int_e [\alpha \mathbf{grad}(\mathbf{u}_\alpha - \mathbf{u}_{\alpha,h}) \mathbf{n} \cdot (J_\varrho^{\frac{1}{2}} \mathbf{v} - \mathbf{v}_h)] \, d\sigma \\
 &= \sum_{K \in T_h} \int_K (\mathbf{f}_h + \alpha_K \Delta \mathbf{u}_{\alpha,h} - \tilde{J}_{\varrho,h} \mathbf{u}_{\alpha,h}) \cdot (J_\varrho^{\frac{1}{2}} \mathbf{v} - \mathbf{v}_h) \, d\mathbf{x} + \int_K (\mathbf{f} - \mathbf{f}_h) \cdot (J_\varrho^{\frac{1}{2}} \mathbf{v} - \mathbf{v}_h) \, d\mathbf{x} \\
 &\quad + \int_K (J_\varrho - \tilde{J}_{\varrho,h}) \cdot (J_\varrho^{\frac{1}{2}} \mathbf{v} - \mathbf{v}_h) \, d\mathbf{x} + \frac{1}{2} \sum_{e \in \mathcal{E}_K} \int_e [\alpha \mathbf{grad}(\mathbf{u}_\alpha - \mathbf{u}_{\alpha,h}) \mathbf{n}_e \cdot (J_\varrho^{\frac{1}{2}} \mathbf{v} - \mathbf{v}_h)] \\
 &= \sum_{K \in T_h} \int_K (\mathbf{f}_h + \alpha_K \Delta \mathbf{u}_{\alpha,h} - \tilde{J}_{\varrho,h} \mathbf{u}_{\alpha,h}) \cdot (J_\varrho^{\frac{1}{2}} \mathbf{v} - \mathbf{v}_h) \, d\mathbf{x} + \int_K (\mathbf{f} - \mathbf{f}_h) \cdot (J_\varrho^{\frac{1}{2}} \mathbf{v} - \mathbf{v}_h) \, d\mathbf{x} \\
 &\quad + \int_K (J_\varrho - \tilde{J}_{\varrho,h}) \cdot (J_\varrho^{\frac{1}{2}} \mathbf{v} - \mathbf{v}_h) \, d\mathbf{x} - \frac{1}{2} \sum_{e \in \mathcal{E}_K} \int_e [\alpha \mathbf{grad} \mathbf{u}_{\alpha,h}] \mathbf{n}_e \cdot (J_\varrho^{\frac{1}{2}} \mathbf{v} - \mathbf{v}_h) \, d\sigma
 \end{aligned}$$

Thus, using the Cauchy-Schwarz inequality, we obtain

(23)

$$\begin{aligned}
 \|\mathbf{u}_\alpha - \mathbf{u}_{\alpha,h}\|_{\varrho,\alpha} &\leq C \left(\sum_{K \in T_h} (\|\mathbf{f}_h + \alpha_K \Delta \mathbf{u}_{\alpha,h} - J_\varrho \mathbf{u}_{\alpha,h}\|_{L^2(K)} \frac{\|J_\varrho^{\frac{1}{2}} \mathbf{v} - \mathbf{v}_h\|_{L^2(K)}}{\|\mathbf{v}\|_{\varrho,\alpha}} \right. \\
 &\quad \left. + \|\mathbf{f} - \mathbf{f}_h\|_{L^2(K)} \frac{\|J_\varrho^{\frac{1}{2}} \mathbf{v} - \mathbf{v}_h\|_{L^2(K)}}{\|\mathbf{v}\|_{\varrho,\alpha}} \right) + h_K \|J_\varrho - \tilde{J}_{\varrho,h}\|_{L^\infty(K)} \frac{\|J_\varrho^{\frac{1}{2}} \mathbf{v} - \mathbf{v}_h\|_{L^2(K)}}{\|\mathbf{v}\|_{\varrho,\alpha}} \\
 &\quad + \frac{1}{2} \sum_{e \in \mathcal{E}_K} \|[\alpha \mathbf{grad} \mathbf{u}_{\alpha,h}] \mathbf{n}_e\|_{L^2(e)} \frac{\|J_\varrho^{\frac{1}{2}} \mathbf{v} - \mathbf{v}_h\|_{L^2(e)}}{\|\mathbf{v}\|_{\varrho,\alpha}} + \frac{|(a_{\alpha,h} - a_\alpha)(\mathbf{v}_{\alpha,h}, \mathbf{u}_{\alpha,h})|}{\|\mathbf{v}\|_{\varrho,\alpha}}.
 \end{aligned}$$

For $K \in \mathcal{T}_h$ we denote by $\mathcal{N}(K)$ the set of its vertices. Let $\mathcal{N}_h = \cup_{K \in \mathcal{T}_h} \mathcal{N}(K)$ be the set of all vertices in \mathcal{T}_h . We denote by $\mathcal{N}_{h,\Omega}$, resp. $\mathcal{N}_{h,\partial\Omega}$, the set of all vertices in Ω , resp. on $\partial\Omega$. For any $K \in \mathcal{T}_h$, $e \in \mathcal{E}_h$ and $x \in \mathcal{N}_h$ we denote by

ω_K the union of all elements sharing an edge e with K ,

$\tilde{\omega}_K$ the union of all elements sharing at least a vertex e with K ,
 ω_e the union of all elements having e as an edge,
 $\tilde{\omega}_e$ the union of all elements sharing at least one vertex with e ,
 ω_x the union of all elements having x as a vertex.

We define the quasi-interpolation operator of Clement type \mathcal{I}_h by

$$\mathcal{I}_h \varphi = \sum_{x \in \mathcal{N}_h, \Omega \cup \mathcal{N}_h, \partial \Omega} \pi_x \varphi \lambda_x$$

where

$$\pi_x \varphi = \frac{1}{|\omega_x|} \int_{\omega_x} \varphi \, dx,$$

is the mean value of φ on ω_x and λ_x the barycentric coordinate associated to x . For vector-valued functions, \mathcal{I}_h is defined by applying it to the components of the function. In particular, $\mathcal{I}_h \mathbf{v} \in \mathbf{V}_h$ for all $\mathbf{v} \in L^2(\Omega)$. For any $\mathbf{v} \in H^1(\Omega)$, $K \in \mathcal{T}_h$ and $e \in E_h$, adapting the argument of [44], we can prove the following interpolation error estimates

$$(24) \quad \begin{aligned} \|\mathbf{v} - \mathcal{I}_h \mathbf{v}\|_{L^2(K)} &\leq c_1 h_K \alpha_K^{-\frac{1}{2}} \|\mathbf{v}\|_{\alpha, \tilde{\omega}_K}, \\ \|\mathbf{v} - \mathcal{I}_h \mathbf{v}\|_{L^2(e)} &\leq c_2 h_e^{\frac{1}{2}} \alpha_e^{-\frac{1}{2}} \|\mathbf{v}\|_{\alpha, \tilde{\omega}_e}, \end{aligned}$$

where c_1, c_2 are constants depending only on the shape parameter.

Proposition 6.3. *For all $K \in \mathcal{T}_h$, $e \in \mathcal{E}_h$ and for all $\mathbf{v} \in \mathbf{V}_\varrho$, there exist $\mathbf{v}_h \in \mathbf{V}_h$ and constants c and c' , independent of h_K and α such that the following estimates hold*

$$(25) \quad \begin{aligned} \|J_\varrho^{\frac{1}{2}} \mathbf{v} - \mathbf{v}_h\|_{L^2(K)} &\leq c h_K \alpha_K^{-\frac{1}{2}} \|\mathbf{v}\|_{\alpha, \tilde{\omega}_K}, \\ \|J_\varrho^{\frac{1}{2}} \mathbf{v} - \mathbf{v}_h\|_{L^2(e)} &\leq c' h_e^{\frac{1}{2}} \alpha_e^{-\frac{1}{2}} \|\mathbf{v}\|_{\alpha, \tilde{\omega}_e}. \end{aligned}$$

The constants c, c' depend on $\lambda_{\min}(J_\varrho^{\frac{1}{2}})$ the lowest eigenvalue of $J_\varrho^{\frac{1}{2}}$ and $\max_{ijk} |(J_\varrho^{\frac{1}{2}})_{ij,k}|$ where we denote by $(J_\varrho^{\frac{1}{2}})_{ij,k}$ the derivative of the coefficient $(J_\varrho^{\frac{1}{2}})_{ij}$ with respect to the variable x_k , $k = 1, 2$.

Proof. Taking $\mathbf{v}_h = \mathcal{I}_h(J_\varrho^{\frac{1}{2}} \mathbf{v})$ and applying the estimates (24), yields

$$\begin{aligned} \|J_\varrho^{\frac{1}{2}} \mathbf{v} - \mathbf{v}_h\|_{L^2(K)} &\leq c_1 h_K \alpha^{-\frac{1}{2}} \|J_\varrho^{\frac{1}{2}} \mathbf{v}\|_{\alpha, \tilde{\omega}_K}, \\ \|J_\varrho^{\frac{1}{2}} \mathbf{v} - \mathbf{v}_h\|_{L^2(e)} &\leq c_2 h_e^{\frac{1}{2}} \alpha^{-\frac{1}{2}} \|J_\varrho^{\frac{1}{2}} \mathbf{v}\|_{\alpha, \tilde{\omega}_e}. \end{aligned}$$

Since $\mathbf{grad}(J_\varrho^{\frac{1}{2}} \mathbf{v}) = J_\varrho^{\frac{1}{2}} : \mathbf{grad} \mathbf{v} + Q \mathbf{v}$, where Q is a third order tensor $Q_{ijk} = (J_\varrho^{\frac{1}{2}})_{ij,k}$, we can write

$$|\mathbf{grad}(J_\varrho^{\frac{1}{2}} \mathbf{v})|_{1, \tilde{\omega}_K} \leq \lambda_{\max}(J_\varrho^{\frac{1}{2}}) |\mathbf{grad} \mathbf{v}| + \max_{ijk} |(J_\varrho^{\frac{1}{2}})_{ij,k}| \lambda_{\min}(J_\varrho^{\frac{1}{2}})^{-1} \|J_\varrho^{\frac{1}{2}} \mathbf{v}\|_{L^2(K)}.$$

which yields the result. \square

Using the inequality [19, Thm7.1]: for all $v \in W^{2,\infty}(K)$,

$$\inf_{q \in P_1} |v - q|_{L^\infty(K)} \leq ch_K^2 |v|_{W^{2,\infty}(K)},$$

we obtain

$$\|J_\varrho - \tilde{J}_{\varrho,h}\|_{L^\infty(K)} \frac{\|J_\varrho^{\frac{1}{2}} \mathbf{v} - \mathbf{v}_h\|_{L^2(K)}}{\|\mathbf{v}\|_{\varrho,\alpha}} = O(\alpha_K^{-\frac{1}{2}} h_K^3).$$

For the term $\frac{|(a_{\alpha,h} - a_\alpha)(\mathbf{v}_h, \mathbf{u}_h)|}{\|\mathbf{v}\|_{\varrho,\alpha}}$ we proceed as in (21), that is,

$$\begin{aligned} (a_\alpha - a_{\alpha,h})(\mathbf{v}_h, \mathbf{u}_{\alpha,h}) &= \sum_{K \in \mathcal{T}_h} \int_K (J_\varrho - J_{\varrho,h}) \mathbf{v}_h \cdot \mathbf{u}_{\alpha,h} \, d\mathbf{x} \\ &\leq \sum_{K \in \mathcal{T}_h} |J_\varrho - J_{\varrho,h}|_{L^\infty(K)} \|\mathbf{v}_h\|_{L^2(K)} \|\mathbf{u}_{\alpha,h}\|_{L^2(K)} \\ &\leq C \sum_{K \in \mathcal{T}_h} \lambda_{\min(J_\varrho)}^{-\frac{1}{2}} h_K |J_\varrho|_{W^{1,\infty}(K)} \|\mathbf{v}_h\|_{L^2(K)} \|J_\varrho^{\frac{1}{2}} \mathbf{u}_h\|_{L^2(K)} \\ &\leq C \lambda_{\min(J_\varrho)}^{-\frac{1}{2}} |J_\varrho|_{W^{1,\infty}(\Omega)} \left(\sum_{K \in \mathcal{T}_h} \|\mathbf{v}_h\|_{L^2(K)}^2 \right)^{\frac{1}{2}} \left(\sum_{K \in \mathcal{T}_h} h_K^2 \|J_\varrho^{\frac{1}{2}} \mathbf{u}_{\alpha,h}\|_{L^2(K)}^2 \right)^{\frac{1}{2}}. \end{aligned}$$

From (22) and an integration by parts, and by adding and subtracting suited terms, we obtain

$$\begin{aligned} \int_\Omega J_\varrho \mathbf{u}_{\alpha,h} \mathbf{u}_{\alpha,h} \, d\mathbf{x} &= \frac{1}{2} \int_\Omega J_\varrho \mathbf{u}_{\alpha,h} \mathbf{u}_{\alpha,h} \, d\mathbf{x} + \frac{1}{2} \sum_{K \in \mathcal{T}_h} \left(\int_K (\mathbf{f}_h + \alpha_K \Delta \mathbf{u}_{\alpha,h} - \tilde{J}_{\varrho,h} \mathbf{u}_{\alpha,h}) \, d\mathbf{x} + \right. \\ &\left. \sum_{e \in \mathcal{E}_K} \int_e \alpha \mathbf{grad} \mathbf{u}_{\alpha,h} \cdot \mathbf{n} \, d\sigma + \int_K (\mathbf{f} - \mathbf{f}_h) \, d\mathbf{x} \right) + \frac{1}{2} \int_\Omega (\tilde{J}_{\varrho,h} - J_\varrho) \mathbf{u}_{\alpha,h} \mathbf{u}_{\alpha,h} \, d\mathbf{x}, \end{aligned}$$

thus, using the definition of η_K (12) and Cauchy-Sscwartz inequality, we deduce

$$\left(\sum_{K \in \mathcal{T}_h} h_K^2 \|J_\varrho^{\frac{1}{2}} \mathbf{u}_{\alpha,h}\|_{L^2(K)}^2 \right) \leq \frac{1}{2} \sum_{K \in \mathcal{T}_h} \alpha_K (\eta_K^2 + h_K^2 \alpha_K^{-1} \|\mathbf{f} - \mathbf{f}_h\|_{L^2(K)}^2) + h.o.t.$$

(h.o.t means a high order term).

From the continuity of the interpolation operator, we have

$$\|\mathbf{v}_h\|_{L^2(K)}^2 \leq C \|\mathbf{v}\|_{L^2(\tilde{\omega}_K)}.$$

Assembling all these estimates yield the proof of (4.1).

6.2. An upper bound for the indicator. We take as a test function $\mathbf{w} \in \mathbf{V}_\varrho$ in (7)

$$\int_\Omega \alpha(\mathbf{x}) \mathbf{grad}(\mathbf{u}_\alpha - \mathbf{u}_{\alpha,h}) : \mathbf{grad} \mathbf{w} \, d\mathbf{x} = \int_\Omega \mathbf{f} \cdot \mathbf{w} \, d\mathbf{x} - \int_\Omega \alpha(\mathbf{x}) \mathbf{grad} \mathbf{u}_{\alpha,h} : \mathbf{grad} \mathbf{w} \, d\mathbf{x} - \int_\Omega J_\varrho \mathbf{u}_{\alpha,h} \cdot \mathbf{w} \, d\mathbf{x}.$$

Integrating by parts yields

$$\begin{aligned} & \int_{\Omega} \alpha(\mathbf{x}) \mathbf{grad}(\mathbf{u}_{\alpha} - \mathbf{u}_{\alpha,h}) : \mathbf{grad} \mathbf{w} \, d\mathbf{x} + \int_{\Omega} J_{\varrho}(\mathbf{u}_{\alpha} - \mathbf{u}_{\alpha,h}) \cdot \mathbf{w} \, d\mathbf{x} = \\ & \sum_{K \in \mathcal{T}_h} \left(\int_K (\mathbf{f} + \alpha_K \Delta \mathbf{u}_{\alpha,h} + J_{\varrho} \mathbf{u}_{\alpha,h}) \cdot \mathbf{w} \, d\mathbf{x} + \int_{\partial K} \mathbf{grad} \mathbf{u}_{\alpha,h} \mathbf{n} \cdot \mathbf{w} \, d\tau \right) \end{aligned}$$

and

$$\begin{aligned} (26) \quad & \int_{\Omega} \alpha(\mathbf{x}) \mathbf{grad}(\mathbf{u}_{\alpha} - \mathbf{u}_{\alpha,h}) : \mathbf{grad} \mathbf{w} \, d\mathbf{x} + \int_{\Omega} J_{\varrho}(\mathbf{u}_{\alpha} - \mathbf{u}_{\alpha,h}) \cdot \mathbf{w} \, d\mathbf{x} = \\ & \sum_{K \in \mathcal{T}_h} \left(\int_K (\mathbf{f} + \alpha_K J_{\varrho} \Delta \mathbf{u}_{\alpha,h} + J_{\varrho} \mathbf{u}_{\alpha,h}) \cdot \mathbf{w} \, d\mathbf{x} - \frac{1}{2} \sum_{e \in \mathcal{E}_K} \int_e [\alpha_K \mathbf{grad} \mathbf{u}_{\alpha,h} \mathbf{n}] \cdot \mathbf{w} \, d\tau \right. \\ & \quad \left. + \int_K (\mathbf{f} - \mathbf{f}_h) \cdot \mathbf{w} \, d\mathbf{x} + \int_K (J_{\varrho} - \tilde{J}_{\varrho,h}) \mathbf{u}_{\alpha,h} \cdot \mathbf{w} \, d\mathbf{x} \right). \end{aligned}$$

We will obtain the estimates by appropriate choices of the function \mathbf{w} in (26)

With each $K \in \mathcal{T}_h$ we associate the bubble function ψ_K equal to the product of the barycentric coordinates on K . For each edge $e \in \mathcal{E}_K$ we associate the bubble function ψ_e equal to the product of the barycentric coordinates on e .

Proposition 6.4. *There exists a constant c independent of h and α such that the following estimate holds for all $K \in \mathcal{T}_h$*

$$(27) \quad \eta_K \leq c \|\mathbf{u}_{\alpha} - \mathbf{u}_{\alpha,h}\|_{\alpha, \omega_K} + c \left(\sum_{K' \in \omega_K} h_{K'}^2 \alpha_{K'}^{-1} \|\mathbf{f} - \mathbf{f}_h\|_{L^2(K')}^2 + h_{K'}^2 \alpha_{K'}^{-1} \|(J_{\varrho} - \tilde{J}_{\varrho,h})^{\frac{1}{2}} \mathbf{u}_{\alpha,h}\|_{L^2(K)}^2 \right).$$

Note that the term $h_{K'}^2 \alpha_{K'}^{-1} \|(J_{\varrho} - \tilde{J}_{\varrho,h})^{\frac{1}{2}} \mathbf{u}_{\alpha,h}\|_{L^2(K)}^2$ is of high order and could be dropped from the estimate (27).

Proof. The proof is performed in two steps.

(1) We take \mathbf{w} in (26) equal to

$$\mathbf{w} = \begin{cases} (\mathbf{f}_h + \alpha_K \Delta \mathbf{u}_{\alpha,h} + \tilde{J}_{\varrho,h} \mathbf{u}_{\alpha,h}) \psi_K & \text{on } K, \\ 0 & \text{elsewhere.} \end{cases}$$

Since ψ_K vanishes on ∂K , this yields

$$\begin{aligned} & \|(\mathbf{f}_h + \alpha_K \Delta \mathbf{u}_{\alpha,h} + \tilde{J}_{\varrho,h} \mathbf{u}_{\alpha,h}) \psi_K^{\frac{1}{2}}\|_{L^2(K)}^2 = \int_K \mathbf{grad}(\mathbf{u}_{\alpha} - \mathbf{u}_{\alpha,h}) : \mathbf{grad}((\mathbf{f}_h + \alpha_K \Delta \mathbf{u}_{\alpha,h} + \tilde{J}_{\varrho,h} \mathbf{u}_{\alpha,h}) \psi_K) \, d\mathbf{x} \\ & - \int_K (\mathbf{f} - \mathbf{f}_h) (\mathbf{f}_h + \alpha_K \Delta \mathbf{u}_{\alpha,h} + \tilde{J}_{\varrho,h} \mathbf{u}_{\alpha,h}) \cdot \psi_K \, d\mathbf{x} - \int_K (J_{\varrho} - \tilde{J}_{\varrho,h}) \mathbf{u}_{\alpha,h} \cdot \psi_K \, d\mathbf{x} \end{aligned}$$

It then follows that

$$\begin{aligned} \|(\mathbf{f}_h + \alpha_K \Delta \mathbf{u}_{\alpha,h} + \tilde{J}_{\varrho,h}) \mathbf{u}_{\alpha,h}\|_{L^2(K)}^2 &\leq \| \mathbf{u}_{\alpha} - \mathbf{u}_{\alpha,h} \|_{\alpha,K} | \alpha_K^{\frac{1}{2}} (\mathbf{f}_h + \alpha_K \Delta \mathbf{u}_{\alpha,h} + \tilde{J}_{\varrho,h} \mathbf{u}_{\alpha,h}) \psi_K |_{H^1(K)} \\ &\quad + \| \mathbf{f} - \mathbf{f}_h \|_{L^2(K)} \| (\mathbf{f}_h + \alpha_K \Delta \mathbf{u}_{\alpha,h} + \tilde{J}_{\varrho,h}) \mathbf{u}_{\alpha,h} \|_{L^2(K)} \\ &\quad + \| (J_{\varrho} - \tilde{J}_{\varrho,h})^{\frac{1}{2}} \mathbf{u}_{\alpha,h} \|_{L^2(K)} \| (\mathbf{f}_h + \alpha_K \Delta \mathbf{u}_{\alpha,h} + \tilde{J}_{\varrho,h}) \mathbf{u}_{\alpha,h} \|_{L^2(K)}. \end{aligned}$$

By going to the reference element, it can be verified that for any polynomial φ of degree at most k the following inequalities hold

$$\| \varphi \|_{L^2(K)} \leq c \| \varphi \psi_K^{\frac{1}{2}} \|_{L^2(K)}, \quad | \varphi \psi_K |_{H^1(K)} \leq c h_K^{-1} \| \varphi \|_{L^2(K)},$$

with the constants depending only on the degree k of the polynomial and on the shape parameter of K . Observing also that ψ_K is ≤ 1 , we obtain

$$(28) \quad h_K \alpha_K^{-\frac{1}{2}} \| (\mathbf{f}_h + \alpha \Delta \mathbf{u}_{\alpha,h} + \tilde{J}_{\varrho,h}) \mathbf{u}_{\alpha,h} \|_{L^2(K)} \leq C (\| \mathbf{u}_{\alpha} - \mathbf{u}_{\alpha,h} \|_{\alpha,K} + h_K \alpha_K^{-\frac{1}{2}} \| \mathbf{f} - \mathbf{f}_h \|_{L^2(K)}) + h_K \alpha_K^{-\frac{1}{2}} \| (J_{\varrho} - \tilde{J}_{\varrho,h})^{\frac{1}{2}} \mathbf{u}_{\alpha,h} \|_{L^2(K)}.$$

(2) Let us denote by e an edge of \mathcal{E}_K , where e is a common edge to two elements K and K' . We take \mathbf{w} in (26) equal to

$$\mathbf{w} = \begin{cases} P_{K,e}([\alpha(\mathbf{x}) \mathbf{grad} \mathbf{u}_{\alpha,h} \mathbf{n}] \psi_e) & \text{on } K, \\ P_{K',e}([\alpha(\mathbf{x}) \mathbf{grad} \mathbf{u}_{\alpha,h} \mathbf{n}] \psi_e) & \text{on } K', \\ 0 & \text{elsewhere.} \end{cases}$$

This yields

$$\begin{aligned} \| [\alpha \mathbf{grad} \mathbf{u}_{\alpha,h} \mathbf{n}] \psi_e^{\frac{1}{2}} \|_{L^2(e)} &\leq \sum_{\kappa \in (K, K')} \| \mathbf{u}_{\alpha} - \mathbf{u}_{\alpha,h} \|_{\alpha,\kappa} | \alpha_{\kappa}^{\frac{1}{2}} P_{\kappa,e}([\alpha \mathbf{grad} \mathbf{u}_{\alpha,h} \mathbf{n}] \psi_e) |_{H^1(K)} \\ &\quad + (\| \mathbf{f}_h + \alpha_{\kappa} \Delta \mathbf{u}_{\alpha,h} + \tilde{J}_{\varrho,h} \mathbf{u}_{\alpha,h} \|_{L^2(\kappa)} + \| \mathbf{f} - \mathbf{f}_h \|_{L^2(\kappa)} \\ &\quad + \| (J_{\varrho} - \tilde{J}_{\varrho,h})^{\frac{1}{2}} \mathbf{u}_{\alpha,h} \|_{L^2(\kappa)}) \| P_{\kappa,e}([\alpha \mathbf{grad} \mathbf{u}_{\alpha,h} \mathbf{n}] \psi_e) \|_{L^2(\kappa)}. \end{aligned}$$

The following inequalities, obtained by going to the reference element hold

$$\begin{aligned} \| [\alpha \mathbf{grad} \mathbf{u}_{\alpha,h} \mathbf{n}] \|_{L^2(e)} &\leq c \| [\alpha \mathbf{grad} \mathbf{u}_{\alpha,h} \mathbf{n}] \psi_e^{\frac{1}{2}} \|_{L^2(e)}, \\ | \alpha_{\kappa}^{\frac{1}{2}} P_{\kappa,e}([\alpha \mathbf{grad} \mathbf{u}_{\alpha,h} \mathbf{n}] \psi_e) |_{H^1(\kappa)} &\leq c h_e^{-\frac{1}{2}} \alpha_{\kappa}^{\frac{1}{2}} \| [\alpha \mathbf{grad} \mathbf{u}_{\alpha,h} \mathbf{n}] \|_{L^2(e)}, \\ h_e^{-1} \| P_{\kappa,e}([\alpha \mathbf{grad} \mathbf{u}_{\alpha,h} \mathbf{n}] \psi_e) \|_{L^2(\kappa)} &\leq c h_e^{-\frac{1}{2}} \| [\alpha \mathbf{grad} \mathbf{u}_{\alpha,h} \mathbf{n}] \|_{L^2(e)}. \end{aligned}$$

Observing that $ch_{\kappa} \leq h_e \leq h_{\kappa}$, we obtain

$$(29) \quad h_e^{\frac{1}{2}} \alpha_e^{-\frac{1}{2}} \| [\alpha \mathbf{grad} \mathbf{u}_{\alpha,h} \mathbf{n}] \|_{L^2(e)} \leq c \sum_{\kappa \in (K, K')} (\| \mathbf{u}_{\alpha} - \mathbf{u}_{\alpha,h} \|_{\alpha,\kappa} + h_e \alpha_e^{-\frac{1}{2}} (\| \mathbf{f}_h + \alpha_{\kappa} \Delta \mathbf{u}_{\alpha,h} + \tilde{J}_{\varrho,h} \mathbf{u}_{\alpha,h} \|_{L^2(\kappa)} + \| \mathbf{f} - \mathbf{f}_h \|_{L^2(\kappa)} + \| (J_{\varrho} - \tilde{J}_{\varrho,h})^{\frac{1}{2}} \mathbf{u}_{\alpha,h} \|_{L^2(K)})).$$

Combining (28) and (29) yields the result. \square

REFERENCES

- [1] L. Alvarez, J. Esclarin, M. Lefebure, and J. Sanchez—A PDE model for computing the optic flow. In Proc. XVI Congreso de Ecuaciones Diferenciales y aplicaciones, Las Palmas de Gran Canaria, Spain (1999), 1349-1346.
- [2] P. Anandan A computational framework and an algorithm for the measurement of visual motion—International Journal of Computer Vision, **39** (1) (2000), 41-56.
- [3] G. Aubert, R. Derriche, P. Kornprobst—Optic flow estimation while preserving its discontinuities: a variational approach, In Proc. Second Asian Conference on Computer Vision, vol **2**, Singapore (1995) 290-295
- [4] G. Aubert, R. Derriche, P. Kornprobst—Computing optical flow via variational techniques, SIAM Journal on Applied Math., **60** (1) (1999), 156-182.
- [5] Z. Belhachmi, C. Bernardi, S. Deparis, F. Hecht—An efficient discretization of the Navier-Stokes equations in an axisymmetric domain. J. Scientific Computing, **27** (1-3) (2006), 97-110.
- [6] Z. Belhachmi, C. Bernardi, A. Karageorghis—Mortar spectral element discretization of nonhomogeneous and anisotropic Laplace and Darcy equations, M2AN, **41**, 4 (2007), 801-824.
- [7] Z. Belhachmi, D. Bucur—Stability and uniqueness for the crack identification problem, SIAM J. Control. Optim. **46**, 1 (2007), 253-273.
- [8] J. Bigün, H. Granlund, J. Wiklund—Multidimensional orientation estimation with applications to textures analysis and optic flow, IEEE Transactions on pattern analysis and machine intelligence, **13**, 8 (1991), 775-790.
- [9] C. Bernardi, R. Verfürth—adaptive finite element methods for elliptic equations with non-smooth coefficients, Numer. Math. **85** (2000), 579-608.
- [10] A. Borzi, K. Ito, K. Kunisch—Optimal control formulation for determining the optical flow, SIAM J. Sci. Computing, **24** (3) (2002), 818-847.
- [11] M. Braack, A. Ern—A posteriori control of modeling errors and discretization errors. Multiscale Model. Simul. **1** (2) (2003), 221-238.
- [12] A. Bruhn—Variational Optic Flow Computation: Accurate Modelling and Efficient Numerics. Ph.D. thesis in Computer Science (2006), Saarland University, Saarbrcken, Germany.
- [13] A. Bruhn, J. Weickert—Confidence measure for variational optic flow methods, In R. Klette, R. Kozera, L. Noakes, and J. Weickert, editors, Geometric Properties from Incomplete Data, Computational Imaging and Vision. Springer, Dordrecht, 2005.
- [14] A. Bruhn, J. Weickert, C. Schnörr—Combining the advantages of local and global optic flow methods, in L. Van Gool Editor, Pattern recognition, Vol **2449** Lecture notes in computer sciences , Springer Berlin (2002), 454-462.
- [15] A. Bruhn, J. Weickert, C. Schnörr— Lucas/Kanade meets Horn/Schunck: Combining local and global optic flow methods. International Journal of Computer Vision, 211-231, (2004).
- [16] A. Bruhn, J. Weickert, C. Feddern, T. Kohlberger, C. Schnörr—Real-time optic flow computation with variational methods, IEEE Transactions on Image Processing, **15** (5) (2005), 608-615.
- [17] P.G. Ciarlet—Basic Error Estimates for Elliptic Problems, in the Handbook of Numerical Analysis, Vol. II, P.G. Ciarlet & J.-L. Lions eds, North-Holland, (1991),17-351.
- [18] I. Cohen—Nonlinear variational method for optical flow computation, In Proc. Eighth Scandinavian Conference on Image Analysis, Tromso, Norway, vol. **1** (1993), 523-530.
- [19] T. Dupont, R. Scott—Polynomial approximation of functions in Sobolev spaces, Math. Comp. **34** (1980), 441-463
- [20] H. Engl, M. Hanke, A. Neubauer—Regularization of inverse problems, Kluwer Acad. Publ. (1996), Dordrecht.

- [21] H. Engl, K. Kunisch, A. Neubauer—Convergence rates for Tikhonov regularization of nonlinear ill-posed problems, *Inverse Problems*, **5** (1989), 523-540
- [22] L. C. Evans—Partial differential equations. Graduate Studies in Mathematics, 19. American Mathematical Society, Providence, RI, 2010 (Second edition).
- [23] V. Girault, P.-A. Raviart—Finite element methods for the Navier-Stokes equations, Theory and algorithms. Springer-Verlag (1986).
- [24] F. Hecht, O. Pironneau—FreeFem++, see www.freefem.org
- [25] W. Hinterberger, O. Scherzer, C. Schnörr, J. Weickert—Analysis of optical flow models in the framework of calculus of variations. *Numerical Functional Analysis and Optimization*, **23** (1/2) (2002), 69-89.
- [26] B. Horn, B. Schunck—Determining optic flow. *Artificial intelligence*, **17** (1981), 185-203.
- [27] C. Kondermann, R. Mester, C. Grabe—Statistical confidence measure for optical flows, *Proc. European Conference on Computer Vision, Lectures Notes in Computer Science*, Vol. **5304**, 290-301, Springer Berlin (2008).
- [28] C. Kondermann, D. Kondermann, B. Jahne, C. Grabe— An adaptive confidence measure for optical flows based on linear subspace projections, *Proc. DAGM Symposium on Pattern recognition, Lectures Notes in Computer Science*, Vol. **4713**, 132-141, Springer Berlin (2007).
- [29] A. Kumar, A.R. Tannenbaum, G. J. Balas—Optic flow: a curve evolution approach, *IEEE Transactions on image processing*, **5**, **4** (1996), 598-610.
- [30] B. Lucas, T. Kanade—An iterative image registration technique with an application to image stereo, *Proc. Seventh international joint conference on artificial intelligence , Vancouver* (1981), 674-679.
- [31] E. Mémin and P. Pérez—A multigrid approach for hierarchical motion estimation. In *Proc. Sixth International Conference on Computer Vision*, 933-938, Bombay, India, 1998. Narosa Publishing House.
- [32] H.H. Nagel—Extending the oriented smoothness constraint into the temporal domain and the estimation of the derivatives of optical flow, In O. Faugeras editor, *Computer vision- ECCV'90*, Vol **427** Lectures notes in computer sciences, Springer Berlin (1990), 139-148.
- [33] H.H. Nagel, W. Enkelmann—An investigation of smoothness constraints for the estimation of displacement vector fields from image sequences , *IEEE Transactions on patterns analysis and machine intelligence* **8** (1986), 565-593.
- [34] H.-G. Roos, M. Stynes, L. Tobiska—Numerical methods for singularly perturbed differential equations. *Convection-diffusion and flow problems. Springer Series in Computational Mathematics*, **24**, Springer-Verlag, Berlin, 1996.
- [35] L.I. Rudin, S. Osher, E. Fatemi—Nonlinear total variation based noise removal algorithms, *Physica D* **60** (1992), 259-268.
- [36] C. Schnörr—Segmentation of visual motion by minimizing convex non quadratic-functionals, In *Proc. Twelfth International Conference on Pattern and Recognition*, volume A, IEEE Computer society press (1994), 661-663
- [37] C. Schnörr—Unique reconstruction of piecewise smooth images by minimizing strictly convex non-quadratic functionals, *Journal of Mathematical Imaging and Vision*, **4** (1994), 189-198.
- [38] M. Sermesant, P. Moireau, O. Camara, J. Sainte-Marie, R. Andriantsimiavona, R. Cimirman, D.L. Hill, D. Chapelle, and R. Razavi—Cardiac function estimation from MRI using a heart model and data assimilation: Advances and difficulties, *Medical Image Analysis*, **10** (4). (2006), 642-656.
- [39] E.P. Simoncelli, E.H. Adelson, D.J. Heeger—Probability distributions of optical flow, *Proc. IEEE Computer Society Conference on Computer Vision and Pattern Recognition* (1991), 310-315.

- [40] D. Shulman, J.-Y. Hervé—Regularization of discontinuous fields, Proc. Workshop on Visual Motion, 81-86, (1989).
- [41] D. Sun, S. Roth, J.M Black—Learning optical flow, Proc. European Conference on Computer Vision, Lectures notes in Computer Science, vol. **5304**, 83-97, Springer, Berlin (2008).
- [42] D. Terzopoulos—Image analysis using multigrid relaxation. IEEE Transactions on Pattern Analysis and Machine Intelligence, **8 (2)**. (1986), 129-139.
- [43] A. N. Tikhonov—Solution of incorrectly formulated problems and the regularization method, Soviet Mathematics Doklady, **4** (1963),1035-1038.
- [44] R. Verfürth—A Review of A Posteriori Error Estimation and Adaptive Mesh-Refinement Techniques, Wiley & Teubner (1996).
- [45] J.Weickert, A.Bruhn, T.Brox, N.Papenberg—A Survey on Variational Methods for Small Displacements, In Mathematical Models for Registration and Applications to Medical Imaging - O. Scherzer (Ed.) Mathematics in Industry, Vol. **10**, Springer, Berlin, 103-136, 2006.
- [46] J. Weickert, C. Schnörr—A theoretical framework for convex regularizers in PDE-based computation of image motion, International Journal of Computer Vision, **45(3)** (2001), 245-264.
- [47] J. Weickert, C. Schnörr—Variational optic flow computations with a spatio-temporal smoothness constraint. Journal of Mathematical Imaging and Vision **14** (2001), 245-255.
- [48] M. Werlberger, W. Trobin, T. Pock, A. Wedel, D. Cremers, H. Bischof—Anisotropic Huber-L1 optical flow, Proc. British Machine Vision Conference.
- [49] H. Zimmer, A. Bruhn, J. Weickert, L. Valgaerts, A. Salgado, B. Rosenhahn, H.P. Seidel—Complementary optical flow, Proc. Energy Minimization Methods in Computer Vision and Pattern Recognition, Lectures Notes in Computer Science, Vol. **5681**, 207-220, Springer Berlin, (2009).

LABORATOIRE DE MATHÉMATIQUES LMAM UMR 7122, UNIVERSITÉ PAUL VERLAINE-METZ , ISGMP, BATIMENT A, ILE DU SAULCY, 57045 METZ, FRANCE.

E-mail address: belhach@univ-metz.fr

LAB. JACQUES-LOUIS LIONS, UNIVERSIT PIERRE ET MARIE CURIE, 175 RUE DU CHEVALERET, 75013 PARIS, FRANCE

E-mail address: hecht@ann.jussieu.fr